Removal of Disinfection Byproducts in Forward Osmosis for Wastewater Recycling

Jiale Xu[1], Thien Ngoc Tran[2], Haiqing Lin[2], Ning Dai[1*]

[1]Department of Civil, Structural and Environmental Engineering
University at Buffalo, The State University of New York, Buffalo, NY, 14260

[2]Department of Chemical and Biological Engineering
University at Buffalo, The State University of New York, Buffalo, NY, 14260

[*]Corresponding author: Post address: 231 Jarvis Hall, Buffalo, NY 14260
Phone: (716) 645-4015; Fax: (716) 645-3667
Email: ningdai@buffalo.edu

Abstract

Forward osmosis (FO) is an emerging membrane technology for wastewater recycling. However, its performance in removing disinfection byproducts (DBPs), a critical aspect of wastewater recycling, has not been investigated. This study systematically investigated the rejection of sixteen neutral DBP that are relevant to wastewater recycling in two commercial FO membranes (Aquaporin and CTA). Clean Aquaporin membrane displayed higher rejection for all DBPs than clean CTA membrane. For *N*-nitrosodimethylamine (NDMA) and haloacetonitriles (HANs), the most prevalent and toxic DBPs in wastewater recycling, the rejection by Aquaporin was 31% and 48%–76%, respectively. The rejection of DBPs in FO positively correlated with their size across different DBP groups but did not correlate with their hydrophobicity. Organic fouling by alginate and bovine serum albumin (BSA) decreased the rejection and transmembrane fluxes of most DBPs. The DBP transport and the influence of fouling were discussed using a solution-diffusion model incorporating size exclusion, the surface interaction between membrane and DBPs, and DBP diffusion within the membrane. Lastly, the rejection of NDMA and HANs in FO membranes determined in this study was compared with that in reverse osmosis (RO) membranes reported in the literature.

Keywords: Forward osmosis (FO), Disinfection byproducts (DBPs), Organic fouling, Wastewater recycling

Highlights:

- Rejection of sixteen disinfection byproducts in forward osmosis (FO) was evaluated.
- Aquaporin membrane exhibited higher rejection to DBPs than CTA membrane.
- Organic fouling decreased the DBP rejection in FO membranes.

1. Introduction

Forward osmosis (FO) is being considered as an alternative or supplement to reverse osmosis (RO) in wastewater recycling [1-3]. FO utilizes the osmotic pressure gradient between wastewater and natural or synthetic saline water to drive water transport through semi-permeable membranes. Examples of FO-based wastewater recycling systems include stand-alone systems using ammonium bicarbonate as the draw solute [4], coupled systems using natural seawater as the draw solution of FO followed by low-pressure RO of diluted seawater [5], and hybrid systems combining electrodialysis and FO [6]. The FO/RO coupled wastewater recycling-seawater desalination system was shown to provide 10%–50% energy saving compared with the RO system [5, 7]. Additionally, because FO does not apply high hydraulic pressure on the feed solution (i.e., wastewater), membrane fouling in FO is more reversible and hence requires less chemical cleaning than RO [8, 9].

The removal of trace organic contaminants, such as pharmaceuticals and personal care products (PPCPs) and disinfection byproducts (DBPs), is critical for wastewater recycling. While PPCPs originate from raw sewage, DBPs are formed when disinfectants are added to wastewater secondary effluents to inhibit membrane biofouling. In RO, PPCP rejection varies with membrane type, fouling, feed solution characteristics, and their physiochemical properties [10-16]. More critically, RO has been shown to poorly reject many DBPs [17, 18], including the trihalomethanes [19-22] regulated by the U.S. Environmental Protection Agency (EPA) [23] and *N*-nitrosodimethylamine (NDMA) [24-32], a nitrogenous DBP imposing 10^{-5} excess cancer risks at a concentration as low as 7 ng/L in drinking water [33]. More than 30 DBPs [17, 34-37] have been detected in full-scale RO-based wastewater recycling plants, with concentrations ranging from 1

ng/L to 100 μg/L. For potable reuse, DBPs represent a higher risk to human health than PPCPs [38, 39].

The rejection of DBPs in FO has not been investigated. Limited studies on the rejection of trace organic contaminants in FO has exclusively focused on PPCPs. The mechanisms for PPCP transport through FO membranes include size exclusion, electrostatic repulsion, and membrane adsorption via electrostatic interaction, hydrophobic interaction, or hydrogen bonding [40-43]. As a result, the FO rejection of PPCPs varies depending on their physiochemical properties. The rejection of positively or negatively charged PPCPs was as high as 70 % [41], but that of nonionic PPCPs varied between 27% to 95% [40, 42]. Hydrophilic and large PPCPs are better rejected than hydrophobic and small PPCPs [41, 43].

Many regulated and emerging DBPs are smaller than PPCPs and do not feature ionizable functional groups, and hence their transport properties would likely differ from those of PPCPs in FO. The difference in rejection behaviors between PPCPs and DBPs have been observed in RO. Most PPCPs were rejected at above 80% by RO membranes [13-15, 44], while the rejection of THMs and nitrosamines were 30%–50% [19-22] and 10%–90% [24-32], respectively. In addition, membrane fouling can significantly influence the rejection of trace organic contaminants, but it is not well understood in FO. Limited studies showed that organic fouling by humic acid and polysaccharides enhanced the FO rejection of ionic PPCPs, but its effects varied for nonionic PPCPs [41, 42].

The objective of this study was to systematically investigate the removal of regulated and emerging DBPs in FO using commercial FO membranes (Aquaporin and CTA). A total of 16 neutral DBPs were studied, including seven nitrosamines, four trihalomethanes (THMs), three haloacetonitriles (HANs), and two haloketones (HKs). The rejection and fluxes of DBPs were

measured for the clean membranes and those fouled by model foulants (alginate or bovine serum albumin (BSA)). Correlation between the FO rejection of DBPs and their molecular size and hydrophobicity was determined. DBP transport mechanisms were then interpreted using a solution-diffusion model. Lastly, the rejection of DBPs in FO obtained from this study was compared with that in RO membranes reported in the literature.

2. Materials and Methods

2.1. Chemicals

The following analytical standards were purchased from Sigma-Aldrich: EPA 521 nitrosamine mix (2000 μg/mL of each nitrosamine in methylene chloride), EPA 501/601 trihalomethanes calibration mix (200 μg/mL of each THM in methanol), and EPA 551B halogenated volatiles mix (2000 μg/ml of each DBP in acetone). *Tert*-butyl methyl ether (MtBE, >99.8%), *N*-nitrosodimethylamine-d_6 (d_6-NDMA, ⩾98%), 1,2-dibromopropane (97%), phosphate buffered saline powder (pH 7.4), BSA (⩾96%), and sodium alginate were provided from Sigma-Aldrich. Methylene chloride (DCM, ⩾99.9%), acetonitrile (HPLC grade, 99.9%), sodium chloride (⩾99.0%), calcium chloride (⩾96%), glycerol (⩾99.5%), and ethyl acetate (⩾99.8%) were supplied by Fisher Chemical. Sodium sulfate (⩾99.0%) and diiodomethane (99%) were provided by Macron, and Alfa Aesar, respectively. All chemicals were used as received. DBP substocks (5 mg/L) were prepared in acetonitrile. All aqueous solutions were prepared using Milli-Q water.

2.2. Membranes

Two commercial FO membranes including Aquaporin (A/S, Lyngby, Denmark) and CTA (Fluid Technology Solutions, Albany, OR, USA) were used in this study. Aquaporin is a new

commercial thin-film composite membrane with aquaporin protein embedded in the polyamide layer. CTA is an asymmetric cellulose triacetate membrane. The investigation of these two membranes' performance in rejecting trace organics to date has been limited to PPCPs [40-43, 45-47]. The characteristics of these two membranes are listed in Table SI-1.

2.3. Forward Osmosis Experiments

A bench-scale cross-flow system (Figure SI-1) was used, which is comprised of a modified permeation cell (SEPA CF II, Sterlitech Corporation) with countercurrent flow for the feed and draw solutions, pressure valves, flow meters, feed and draw solution reservoirs, and two gear pumps (Cole Parmer), as previously described [48, 49]. The permeation cell holds a membrane with an effective area of 140 cm^2 and features 2 mm channel height on each side.

Before the experiments, the FO membranes were immersed in Milli-Q water for 24 h. At the beginning of the experiments, the draw and feed reservoirs contain 1.5 L of 1 M NaCl solution and 1.5 L Milli-Q water, respectively. Crossflow velocity was set at 0.048 m/s. After the FO system reached constant water flux (approximately 15 min), DBPs were spiked into the feed reservoir to make up an initial concentration of 10 μg/L for nitrosamines or 20 μg/L for halogenated DBPs. The concentration of halogenated DBPs used in the experiments was in the range relevant to wastewater, whereas that of nitrosamines was 10-100 times higher than the typical values in wastewater for the ease of detection. The feed and draw reservoirs were sampled every hour (5 and 15 ml, respectively) for DBP analysis. The volume of feed and draw solutions was recorded continuously based on the weight of the reservoirs. The volume of samples withdrawn for DBP analysis was accounted for during data processing. The conductivity and pH of both draw and feed solutions were measured before and after the experiments.

To investigate the effect of organic fouling on DBP rejection, sodium alginate and BSA were used as model foulants. The fouling layer was established using feed solutions containing one of the foulants at 1 g/L. Alginate solutions were conditioned using 50 mM NaCl and 0.5 mM $CaCl_2$, and BSA solutions were buffered by 0.01 M phosphate buffer at pH 7.4. A higher concentration of NaCl draw solution (1.5 M) was used to accelerate fouling. A control experiment was conducted in the absence of the foulants to account for the flux decline due to the dilution of the draw solution over time. After 15 h, a new feed solution containing a lower concentration of foulant (0.2 g/L) and DBPs was used, and the draw solution was replaced with a fresh 1 M NaCl solution to test DBP rejection, following the same procedures described above. The purpose of adding 0.2 g/L of foulant to feed solution is to prevent the dissolution of fouling into the bulk solution. Water fluxes were compared between the fouling and control experiments when the same volume of water had permeated through, and the difference was indicative of the extent of fouling on the membranes.

The calculation of water and DBP fluxes, DBP rejection, and DBP permeance is described in Text SI-1. Concentration polarization factor (β) was calculated as described in Text SI-2. Table SI-2 showed the values of β for all sixteen DBPs in clean Aquaporin and CTA membrane experiments in this study.

2.4. DBP Analysis

Nitrosamines were solvent-extracted using DCM. Feed solution samples (5 mL) were diluted to 15 mL by Milli-Q water before extraction. Deuterated standard d_6-NDMA was used as an internal standard. DCM extracts were analyzed using gas chromatography-mass spectrometry (Agilent 7890B GC-240 Ion Trap MS) with a VF-5ms column. The GC-MS method was the same as previously reported [50]. Halogenated DBPs were extracted with MtBE. Samples (15 mL) were

spiked with the internal standard 1,2-dibromopropane and mixed with 2 mL MtBE and 5 g sodium sulfate. The MtBE extracts were analyzed by GC-electron capture detector (Agilent 7890B-^{63}Ni ECD) with a HP-5 column. The GC-ECD method is as follows: 3 μL splitless injection at 150 ºC; column temperature was held at 26 °C for 9 min, then raised to 60 °C at 25 °C/min and held for 1 min, and then raised to 100 °C at 20 °C/min and held for 1 min, and then raised to 250 °C at 70 °C/min and held for 1 min; ECD temperature was 290 ºC, and the makeup gas was a mixture of methane and argon with a flow rate of 18.8 mL/min.

2.5. Membrane Characterization

The hydrophobicity of the membrane surface was evaluated using a contact angle goniometer (Model 190, Rame-Hart Instrument Co.) with Milli-Q water as the probing liquid. The surface tension (γ_i, mJ/m^2) of a membrane is expressed as

$$\gamma_i = \gamma_i^{LW} + 2\sqrt{\gamma_i^+ \gamma_i^-} \tag{1}$$

where γ_i^{LW} is the apolar (Lifshitz-van der Waals) component, and γ_i^+ and γ_i^- are the polar (Lewis acid-base) electron-accepting and electron-donating components, respectively [51]. The subscript *i* stands for liquid solvent (L), membrane (M), or water (W). The specific components of membrane surface tension are linked to the contact angle (θ) of a droplet of liquid on the membrane via the Young-Dupré equation [51]:

$$(1+\cos\theta)\gamma_L = 2\left(\sqrt{\gamma_M^{LW}\gamma_L^{LW}} + \sqrt{\gamma_M^+\gamma_L^-} + \sqrt{\gamma_L^+\gamma_M^-}\right) \tag{2}$$

γ_M^{LW}, γ_M^+, and γ_M^- were determined by solving equation 2 using the contact angles of a nonpolar solvent (diiodomethane), and two polar solvents (glycerol and water) [52-54].

The clean and fouled membranes were also examined by focused ion beam-scanning electron microscope (FIB-SEM, Zeiss Auriga). Before imaging, membrane samples were coated

with a thin gold film (2–5 nm) by electron-beam evaporation deposition (AXXIS, Kurt J. Lesker Co.) to eliminate the charging effect on the samples during the surface imaging.

3. Results and Discussion

3.1. Rejection of DBPs in FO by Clean Membranes

Table 1 summarizes the physiochemical properties of the DBPs investigated in this study. Eighteen DBPs were initially selected for evaluation, but only sixteen are discussed below, because two of the DBPs, TCAN and TCNM, hydrolyzed rapidly in aqueous solutions. In an aqueous solution, 80% of the initial TCAN and TCNM mass degraded over 12 h (Figure SI-2). Therefore, their concentrations in the feed and draw solutions during the membrane experiments (8 h) were not indicative of their rejection. The fast hydrolysis of TCAN and TCNM has been reported previously in Milli-Q water [19, 55, 56]. For the other sixteen DBPs, hydrolysis, volatilization, or sorption loss was insignificant (total mass recovery 75%–97%, as shown in Figure SI-2). In wastewater recycling for potable reuse, NDMA and haloacetonitriles (HANs) are the most problematic DBPs due to their significant formation from wastewater organic matter, high toxicity, and, in the case of HANs, persistence in advanced oxidation processes [17]. Therefore, the discussion below will place more emphasis on these DBPs when appropriate.

Table 1. Disinfection byproducts (DBPs) investigated in this study. MW=molecular weight (g/mol), MV=molecular volume (Å^3), D=Stokes diffusion coefficient ($\times 10^{-10}$ m^2/s), C_{cancer}=concentration in drinking water that corresponds to 10^{-6} excess cancer risks (μg/L), and LD_{50}=cytotoxicity lethal dose at 50% death rate (M).

Name		Abbrev.	MW[a]	MV[b]	log K_{ow}[a]	D[c]	C_{cancer}[d]	LD_{50}[e]
Nitrosamines								
N-nitrosodimethylamine		NDMA	74	73	-0.64	8.27	7×10^{-4}	–
N-nitrosomethylethylamine		NMEA	88	90	-0.15	7.72	2×10^{-3}	–
N-nitrosodiethylamine		NDEA	102	107	0.34	7.28	2×10^{-4}	–
N-nitrosodi-*n*-propylamine		NDPA	130	141	1.33	6.64	5×10^{-3}	–
N-nitrosodi-*n*-butylamine		NDBA	158	174	2.31	6.19	6×10^{-3}	–
N-nitrosopyrrolidine		NPYR	100	97	0.23	7.53	2×10^{-2}	–
N-nitrosopiperidine		NPIP	114	113	0.72	7.15	–	–
Halogenated DBPs								
Trihalomethane	Chloroform	TCM	119	70	1.97	8.39	–	9.17×10^{-3}
(THM)	Bromodichloromethane	DCBM	164	75	2.00	8.20	–	1.15×10^{-2}
	Dibromochloromethane	DBCM	208	79	2.16	8.06	–	5.36×10^{-3}
	Bromoform	TBM	253	83	2.40	7.93	–	3.96×10^{-3}
Haloactonitrile	Dichloroacetonitrile	DCAN	110	73	0.29	8.27	–	5.73×10^{-5}
(HAN)	Bromochloroacetonitrile	BCAN	154	77	0.38	8.13	–	8.46×10^{-6}
	Dibromoacetonitrile	DBAN	199	82	0.47	7.96	–	2.85×10^{-6}
	Trichloroacetonitrile	TCAN	144	87	2.09	7.80	–	1.60×10^{-4}
Haloketone	1,1-Dichloro-2-propanone	1,1-DCP	127	92	0.20	7.66	–	–
(HK)	1,1,1-Trichloro-2-propanone	1,1,1-TCP	161	107	1.12	7.28	–	–
Halonitromethane (HNM)	Chloropicrin	TCNM	164	93	2.09	7.63	–	5.36×10^{-4}

a Source: http://www.chemspider.com/.
b Source: ACD/Percepta Platform Version 2016.1.
c Calculated based on equation 6.
d [33].
e [57].

DBP rejection in FO was first evaluated in the absence of any foulants. Over the course of the experiments (8 h), water fluxes for Aquaporin and CTA membranes remained constant at 8.1 and 6.0 L/(m^2·h), respectively (Table SI-1). For most DBPs, the rejection declined after system startup (Figure SI-3). Aquaporin and CTA reached the stabilized DBP rejection after 600 and 400 mL water permeated through the membranes (4 h), respectively. The stabilized rejection is used in the following discussion.

Figure 1 shows the rejection of DBPs by the two membranes. Aquaporin membrane displayed higher rejection than CTA membrane, by a factor of 1.7–7.0, 2.3–8.9, 2.1–13, and 1.5–3.4 for nitrosamines, THMs, HANs, and HKs, respectively. The rejection of NDMA by Aquaporin and CTA was 31% and 4%, respectively; and the rejection of HANs was 48%–76%, and 4%–36%, respectively. Overall, these high priority DBPs were not well rejected.

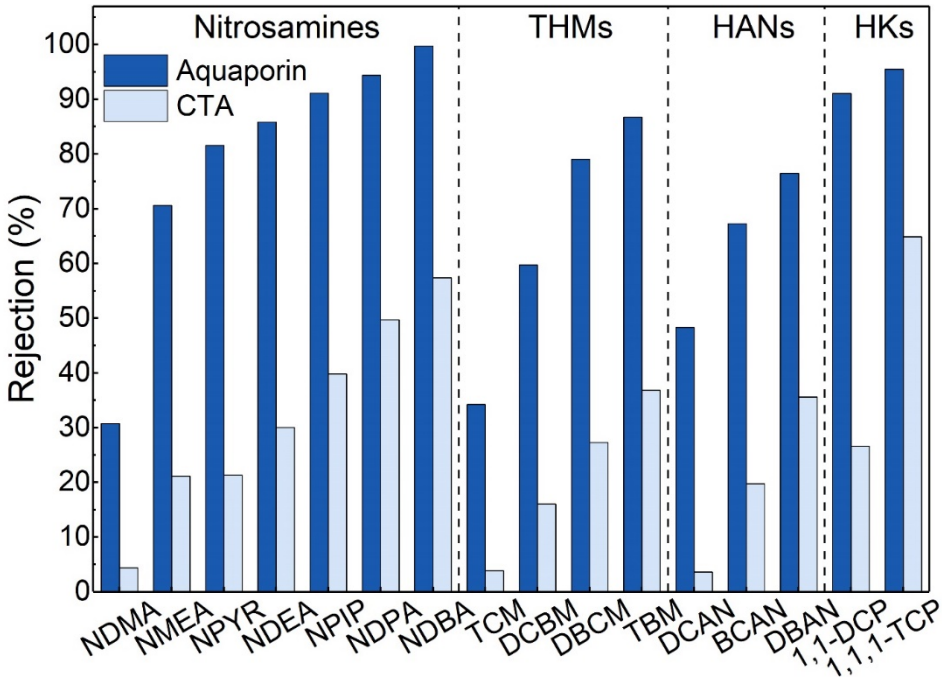

Figure 1. Stabilized FO rejection of DBPs by Aquaporin and CTA membranes at 21 °C. Water fluxes for Aquaporin and CTA membranes are 8.1 and 6.0 L/(m^2·h), respectively; draw solution 1 M NaCl; nitrosamine concentration 10 µg/L; halogenated DBP concentration 20 µg/L; and pH 6.5–7.5.

Figure 2 shows the relationship between the FO rejection of DBPs and their size (molecular volume) or hydrophobicity (log K_{ow}). Molecular volume was used as an indicator of molecular size instead of the more commonly used molecular weight because brominated and chlorinated DBPs of similar sizes have drastically different molecular weight (Table 1). When Pearson's (linear) and Spearman's (monotonic) correlations were evaluated for all sixteen DBPs (Table SI-3), statistically significant and positive correlations were observed between DBP rejection and molecular volume for both membranes ($p < 0.05$), but not between DBP rejection and log K_{ow} values. Nitrosamine rejection appears to increase with log K_{ow}, but the correlation is inconclusive due to the covariance of hydrophobicity and molecular volume. Hydrophobic DBPs are anticipated to be preferentially adsorbed on the polymeric membrane surface, thereby featuring higher transport and lower rejection than the more hydrophilic DBPs (of similar sizes). However, this could not explain the comparable rejection of THMs and HANs, two groups of DBPs with drastically different hydrophobicity (Figures 2c and 2d). It is likely that additional interaction mechanisms such as hydrogen bonding plays a role in the partition of solute on membrane surface [19]. HANs feature a hydrogen bond acceptor site (the nitrile group) that is absent in THMs.

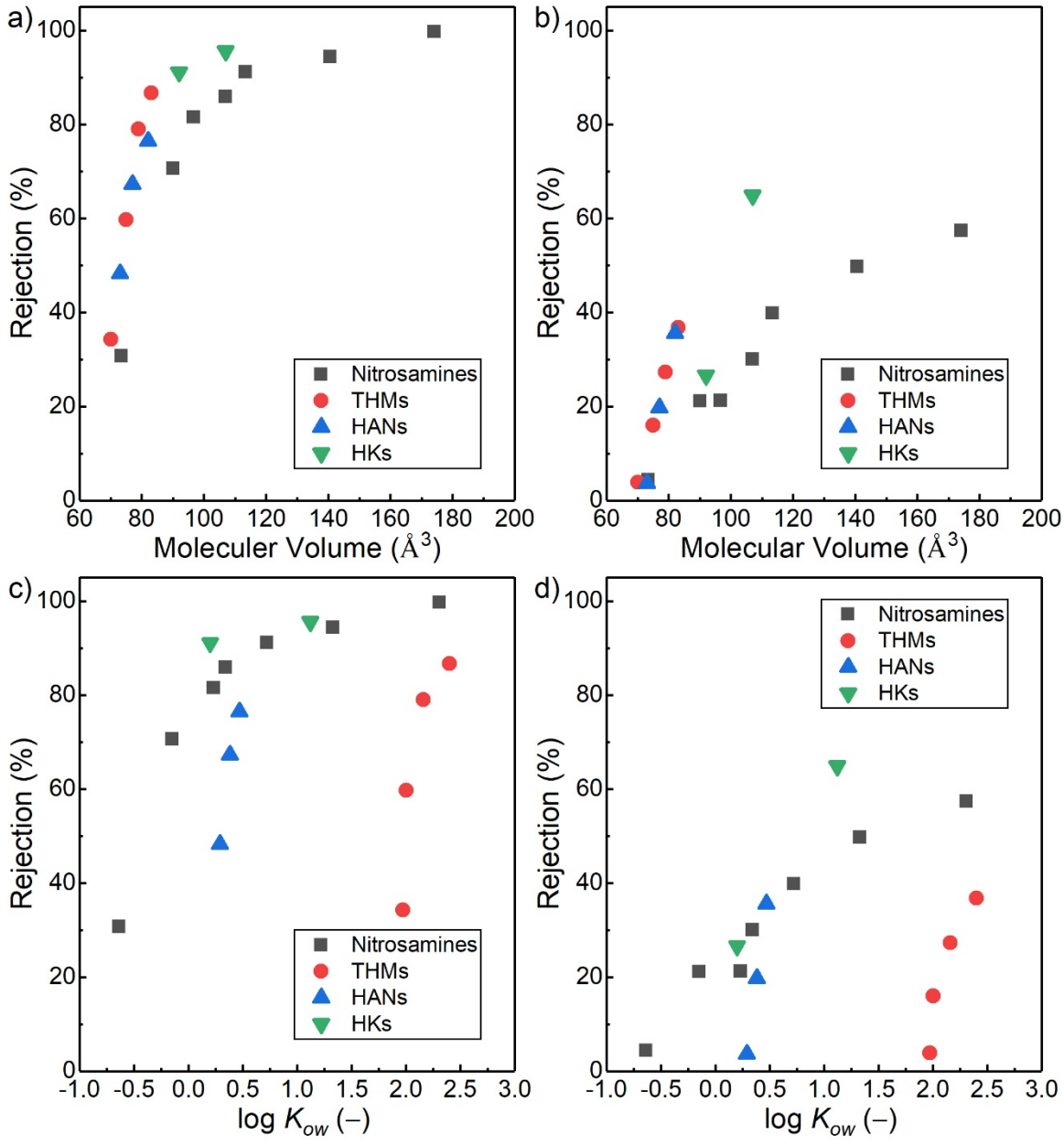

Figure 2. Stabilized rejection of DBPs by (a and c) Aquaporin and (b and d) CTA membranes in relation to (a and b) molecular volume and (c and d) log K_{ow}.

Because DBP rejection was influenced by water fluxes, DBP fluxes were calculated to directly quantify DBP transport and used to compare the two membranes (Figure 3). CTA membrane has higher fluxes than Aquaporin for most DBPs with a factor of 1.1–6.6 difference. NDMA flux was similar in the two membranes, but the flux of HANs through CTA was 1.4–2.0

times higher than that through Aquaporin. The flux of DBPs decreased with their molecular volume for both membranes (Figure SI-4). DBP permeance was compared in Figure SI-5. Aquaporin membrane exhibited 1.6–10 times lower permeance for all DBPs than CTA membrane.

Lastly, it is worth mentioning that we evaluated DBP rejection in FO using unbuffered solutions constituted in Milli-Q water, but the solution pH range (6.5–7.5) lies within the normal range of pH for wastewater (6.8–7.7 [58]). We expect that the DBP rejection determined using the low ionic strength feed solutions is comparable to that using authentic wastewater, because previous nanofiltration (NF) and RO studies [19, 24, 26] have shown that DBP transport is not affected by ionic strength in the range relevant to wastewater (< 20 mM [58]).

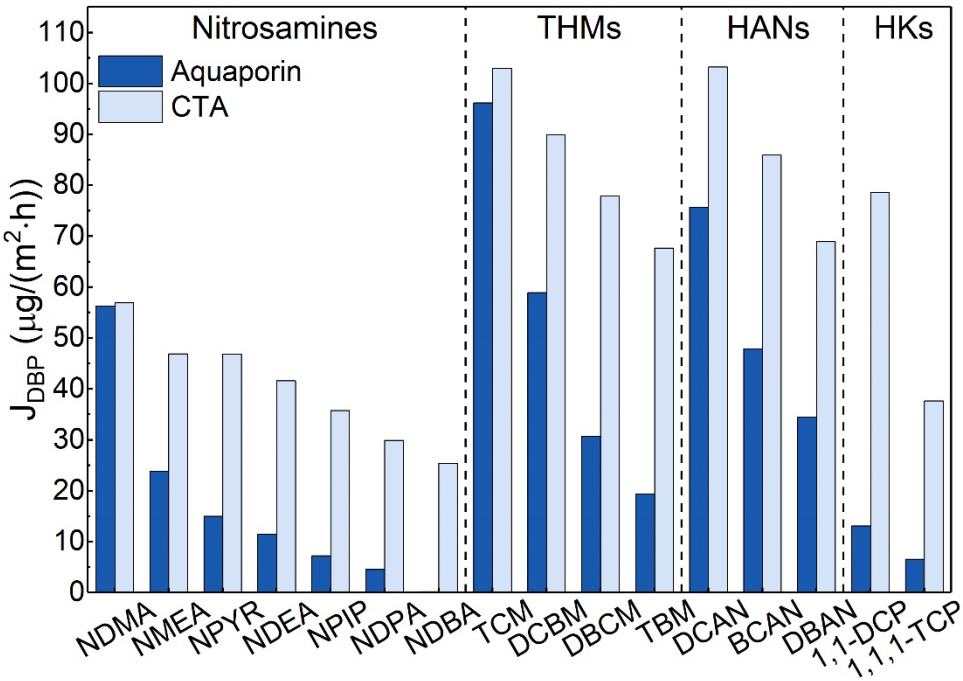

Figure 3. DBP fluxes of DBPs by Aquaporin and CTA membranes. Experimental conditions are as introduced in the caption of Figure 1.

3.2. Influence of Organic Fouling on DBP Rejection and Transmembrane Fluxes

Alginate and BSA are model foulants representing the polysaccharide and protein components of the extracellular polymeric substances in treated wastewater, respectively. In our experiments, fouling layers were established on the membranes after 15 h, as indicated by the water flux decline (Figure SI-6) and the surface SEM images (Figure SI-7). The decline in water fluxes by alginate and BSA was similar, in the range of 35%–42% (Figure SI-8). Aquaporin exhibited water permeance 1.2–1.6 times higher than CTA (Figure SI-8). During the DBP rejection experiments, water fluxes of the fouled membranes remained relatively constant. DBP rejection by the fouled membranes declined after the system startup, similar to that observed for clean membranes, but it was stabilized after a lower water transport volume (300–400 mL; Figure SI-9 as an example).

Figures 4a and 4b show the stabilized rejection of DBPs by the alginate- and BSA-fouled membranes, respectively. Similar to that observed for clean membranes, Aquaporin displayed higher DBP rejection than CTA for all DBPs. The relative rejection of different DBPs by the same membrane was not altered by fouling (Figures 1 and 4). The rejection of NDMA by the alginate- and BSA-fouled Aquaporin membranes was 34% and 16%, respectively, and the rejection of HANs was 36%–58% and 24%–38%, respectively. In this study, we used foulant concentrations higher than those typically experienced in wastewater recycling to accelerate the formation of fouling layer on the membranes, and to form a thicker layer to assess the worst-case scenario regarding the effect of fouling on DBP rejection. As shown in Figures 4c and 4d, organic fouling decreased the rejection of most DBPs, and a more dramatic decrease was observed for Aquaporin. The only exception is the increase in rejection of the relatively small nitrosamines, including NDMA, by CTA membrane after alginate fouling. The decrease in HAN rejection by Aquaporin was twice more pronounced after the BSA fouling than that after the alginate fouling.

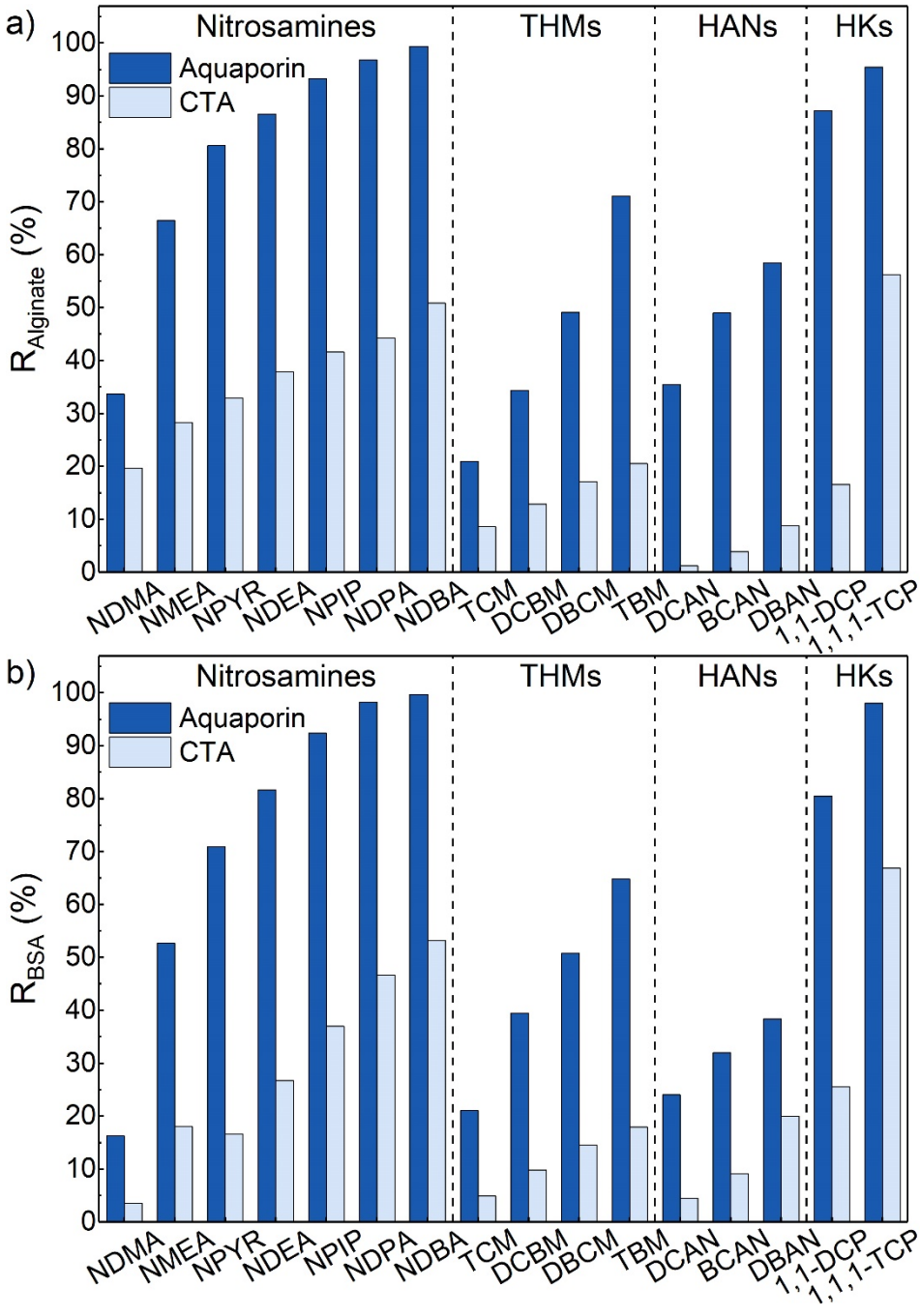
a)
Nitrosamines
THMs
HANs
HKs
Aquaporin
CTA
$R_{Alginate}$ (%)
0
10
20
30
40
50
60
70
80
90
100
NDMA
NMEA
NPYR
NDEA
NPIP
NDPA
NDBA
TCM
DCBM
DBCM
TBM
DCAN
BCAN
DBAN
1,1-DCP
1,1,1-TCP
b)
Nitrosamines
THMs
HANs
HKs
Aquaporin
CTA
R_{BSA} (%)
0
10
20
30
40
50
60
70
80
90
100
NDMA
NMEA
NPYR
NDEA
NPIP
NDPA
NDBA
TCM
DCBM
DBCM
TBM
DCAN
BCAN
DBAN
1,1-DCP
1,1,1-TCP

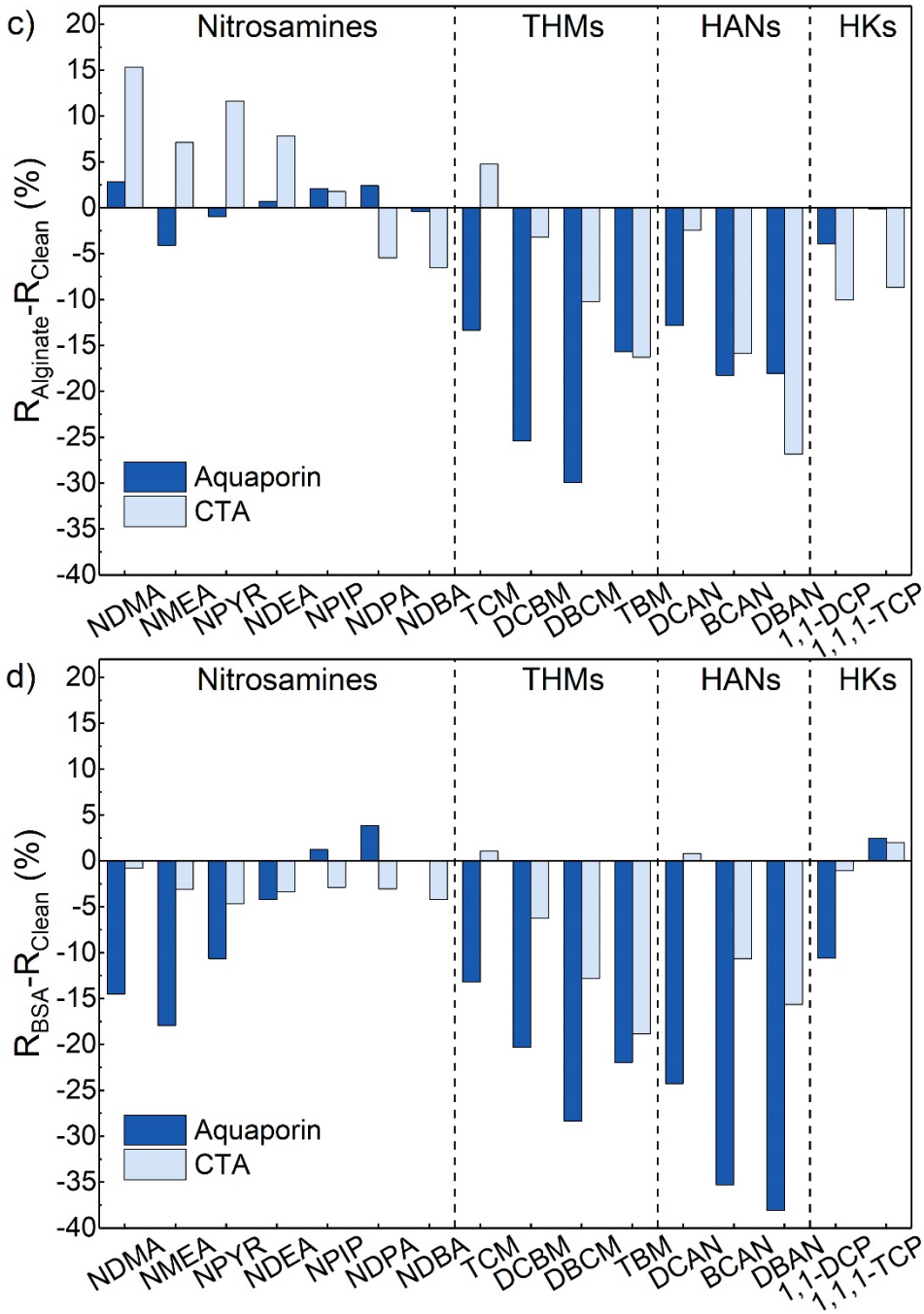

Figure 4. Stabilized rejection of DBPs by (a) alginate- and (b) BSA-fouled membranes at 21 °C; comparison of DBP rejection by clean membranes and (c) alginate- or (d) BSA-fouled membranes. R = stabilized rejection. Water fluxes for alginate-fouled membranes were 5.7 and 3.6 L/(m^2·h) for Aquaporin and CTA, respectively; water fluxes for BSA-fouled membranes were 3.8 and 3.2 L/(m^2·h) for Aquaporin and CTA, respectively; draw solution 1 M NaCl; nitrosamine concentration 10 µg/L; halogenated DBP concentration 20 µg/L; solution pH 6.5–7.5.

After fouling, the transmembrane flux of most DBPs in Aquaporin remained lower than that in CTA (Figure SI-10). Exceptions were observed for NDMA, TCM, DCBM, and DCAN in the alginate-fouled membranes, where Aquaporin exhibited higher fluxes than CTA. As shown in Figure SI-10c and 10d, organic fouling tends to decrease DBP flux. NDMA flux was reduced by 32%–49%. For HANs, their fluxes through CTA decreased by 14%–47% after fouling, but their fluxes through Aquaporin varied depending on the HAN species: DCAN fluxes decreased by 12%–32%, but DBAN fluxes increased by 22%–25%. Similar variability was observed for the fluxes of THMs through Aquaporin.

3.3. DBP Transport Mechanisms in FO

The solution-diffusion model is commonly used to describe the transport of organic compounds such as PPCPs in nanofiltration [52, 53, 59-61], RO [62-64], and FO membranes [45, 46, 54] based on their physiochemical properties and membrane characteristics [65]. For Aquaporin membrane, the presence of aquaporin protein channels opens the possibility for "pore flow", especially when considering water fluxes [66]; however, previous studies showed that the transport of organic compounds through Aquaporin was largely governed by the polyamide matrix instead of the aquaporin channels [45, 46]. Therefore, we hypothesized that DBP transport through FO membranes can be modeled using the solution-diffusion model, in which the sorption of DBPs on the membrane surface is followed by diffusion through the membrane (Figure SI-11a).

The flux of DBPs is related to their permeance through the membrane and the concentration polarization adjacent to the membrane surface:

$$J_{DBP} = B_{DBP}(\beta C_F - C_D) \quad (3)$$

where B_{DBP} (m/s) is the permeance of DBP through the membrane, β is the concentration polarization factor calculated as described in Text SI-2, and C_F (μg/L) and C_D (μg/L) are the DBP concentration in the feed and draw solutions, respectively.

Polyamide and cellulose triacetate layers are "nonporous" in the classical solution-diffusion model. However, previous studies [46, 64, 67] showed these dense layers contained interconnected pore-like "microvoids" with an effective average pore radius in the range of 0.2–0.4 nm. Hence, Aquaporin and CTA membranes contain hypothetical cylindrical pores with an effective pore radius (r_p, mean average of membrane pore radii). DBP permeance can be calculated as [65]:

$$B_{DBP} = (1-\lambda)^2 \exp\left[-\left(\frac{\Delta G_{DBP,M}}{kT}\right)\right]\frac{D_{DBP,M}\varepsilon}{\Delta x} \quad (4)$$

where λ (= r_s/r_p) is the ratio of the molecular radius (r_s, m) of a DBP to r_p (m) of a membrane, $\Delta G_{DBP,M}$ (J) is the free energy of the DBP-membrane surface interaction for one DBP molecule, $D_{DBP,M}$ (m^2/s) is the diffusion coefficient of a DBP within a membrane, $\Delta x/\varepsilon$ (m) is the ratio of the membrane thickness to porosity, k is the Boltzmann constant (1.38×10^{-23} $m^2 \cdot kg/(s^2 \cdot K)$), and T is the temperature (K).

The three terms of $(1-\lambda)^2$, $\exp[-(\Delta G_{DBP,M}/kT)]$, and $D_{DBP,M}\varepsilon/\Delta x$ represent the influence of the size exclusion, DBP–membrane surface interaction, and DBP diffusion within the membrane on DBP transport, respectively. The values of r_p and $\Delta x/\varepsilon$ for Aquaporin and CTA were obtained by solving equation 4 for two reference organic solutes, glycerol and ethyl acetate. The details are shown in Text SI-3. $\Delta G_{DBP,M}$ can be estimated using the surface tension components of the membrane, water, and DBP [51, 52]:

$$\Delta G_{DBP,M} = 2A_{DBP}\left[\begin{array}{l}\sqrt{\gamma_{DBP}^{LW}\gamma_L^{LW}} + \sqrt{\gamma_M^{LW}\gamma_L^{LW}} - \sqrt{\gamma_M^{LW}\gamma_{DBP}^{LW}} - \gamma_L^{LW} + \sqrt{\gamma_L^+}\left(\sqrt{\gamma_{DBP}^-} + \sqrt{\gamma_M^-} - \sqrt{\gamma_L^-}\right) \\ +\sqrt{\gamma_L^-}\left(\sqrt{\gamma_{DBP}^+} + \sqrt{\gamma_M^+} - \sqrt{\gamma_L^+}\right) - \sqrt{\gamma_{DBP}^+\gamma_M^-} - \sqrt{\gamma_{DBP}^-\gamma_M^+}\end{array}\right] \quad (5)$$

where A_{DBP} (= $\pi r_s^2/2$) is the contact area between a DBP molecule and the membrane [52, 68]. The surface tension components are introduced in equation 1. $D_{DBP,M}$ (= $K_d D_L$) can be estimated by incorporating the diffusion coefficient (D_L, m^2/s) of DBP in water and the membrane diffusion hindrance factor (K_d) [52]. D_L was calculated by the Stokes–Einstein equation:

$$D_L = \frac{kT}{6\pi\mu r_s} \tag{6}$$

where μ (Pa·s) is the dynamic viscosity of water. K_d was calculated as follows [69]:

$$K_d = \frac{6\pi}{\frac{9}{4}\pi^2\sqrt{2}(1-\lambda)^{-5/2}\left[1+\sum_{n=1}^{2}a_n(1-\lambda)^n\right]+\sum_{n=0}^{4}a_{n+3}\lambda^n} \tag{7}$$

where the constants of a_n are shown in Table SI-4. The obtained values of K_d of TCM and TBM in Aquaporin and CTA are shown in Table SI-5.

Because the surface tension components of DBPs are only available for chloroform (TCM) [70] and bromoform (TBM) [71], the preliminary modeling attempt is limited to these two DBPs. The surface tension components for Aquaporin and CTA membranes were calculated based on the contact angle measurements (Figure SI-12). $\Delta G_{DBP,M}$ values (Table SI-6) for TCM and TBM were calculated using equation 5.

Table 2 summarizes the permeance of TCM and TBM estimated by equation 4 and the values of the three terms. The estimated TCM permeance was 6.6 and 2.3 times higher than TBM permeance through Aquaporin and CTA membranes, respectively. The lower size exclusion and higher diffusivity of TCM are the dominant causes for its higher permeance than TBM. The $(1-\lambda)^2$ and $D_{DBP,M}\varepsilon/\Delta x$ terms of TCM is 1.5–2.5 and 1.9–3.5 times larger than TBM, respectively. TBM interacts with the membrane surface more favorably than TCM, due to the greater hydrophobicity of TBM. The model predicts CTA to be 2.7–7.8 times more permeable than Aquaporin to TCM and TBM, attributable to the larger effective pore size of CTA (0.333 nm) than

Aquaporin (0.297 nm), and the stronger surface interaction of TCM and TBM with CTA than with Aquaporin.

Table 2. DBP permeance and relevant terms in DBP membrane transport.

Membrane properties		DBP	Size exclusion $(1-\lambda)^2$ ($\times 10^{-3}$)	Membrane surface adsorption $\exp[-(\Delta G_{DBP,M}/kT)]$ (–)	DBP diffusion in membrane $D_{DBP,M}\varepsilon/\Delta x$ ($\times 10^{-5}$ m/s)	DBP permeance B_{DBP} ($\times 10^{-6}$ m/s)
Name	r_p[a] (nm)					
Aquaporin	0.297	TCM	19.1	2.39	3.48	1.59
		TBM	7.7	3.10	1.00	0.24
CTA	0.333	TCM	53.5	3.28	2.48	4.35
		TBM	34.7	4.07	1.33	1.88

[a] Calculated based on Text SI-3.

Using the model-predicted permeance of TCM and TBM, their fluxes and rejection can be calculated from the experimentally determined concentration polarization factor, DBP concentration, and water flux (equation 3). Table 3 compares the modeled fluxes and rejection with the experimentally determined values. The model overestimated DBP fluxes by 1.6–1.9 times and 2.4–3.5 times for Aquaporin and CTA, respectively, and even predicted negative rejection. These results suggest that there are other processes influencing DBP transport through FO membranes that are not accounted for by the model. Previous studies suggest that retarded forward diffusion, induced by the reverse salt flux, may decrease the transport of organic solutes such as neutral PPCPs through FO membranes [40, 67]. This would be consistent with the greater extent of overestimation of DBP flux through CTA, which featured twice higher reverse salt flux than Aquaporin (Table SI-1). Considering that the radii of TCM and TBM (0.256 and 0.271 nm) were comparable to the hydrated radii of Na^+ (0.36 nm) and Cl^- (0.33 nm) [72], and that the reverse NaCl flux (3.5–5.5 g/(m^2·h)) was 10^5 times higher than the forward DBP flux (19–103 μg/(m^2·h))

in our experiments, it is likely that considering reverse salt flux will improve model accuracy. Work is ongoing to further investigate the role of reverse salt flux on DBP transport through FO membranes, and to expand the modeling to the high priority DBPs such as NDMA and HANs.

Table 3. Comparison between experimental and modeled DBP (a) flux and (b) rejection of TCM and TBM. Experimental conditions are introduced in Figure 1. Concentration polarization factors of TCM and TBM for clean Aquaporin and CTA membranes are shown in Table SI-2, and are used in calculating both experimental and modeled J_{DBP} (equation 3). Rejection was calculated using experimentally determined water flux. The negative rejection predicted from the model is due to an overestimation of DBP flux, as discussed in the text.

Membrane	DBP	Experimental J_{DBP} (μg/(m^2·h))	Modeled J_{DBP} (μg/(m^2·h))	Experimental R (%)	Modeled R (%)
Aquaporin	TCM	96	185	34	-26
	TBM	19	31	87	79
CTA	TCM	103	358	4	-234
	TBM	68	164	37	-53

DBP transport through the fouled membranes can be described by a similar conceptual model (Figure SI-11b). The influence of fouling on DBP fluxes are the net effects of three processes. First, fouling can hinder the back diffusion of DBPs from the membrane surface to the bulk solution, increasing concentration polarization that leads to higher DBP fluxes and lower rejection [42, 73]. Second, fouling can affect DBP permeance by modifying the surface properties of membranes, the extent and nature of which depend on the type of the foulants and membranes. As shown in Figure SI-12, the water contact angles of FO membranes increased by 1.4–3.6 times after fouling, suggesting that the fouled surfaces were much more hydrophobic and likely had a stronger interaction with DBPs. Lastly, when a compact fouling layer is formed on the membrane surface, it can reduce the effective pore radius of the membrane [20], and thereby decrease DBP flux and increase rejection.

As shown in the Figure SI-10, the fluxes of most DBPs decreased, suggesting that neither enhanced concentration polarization or the change in DBP-membrane surface interaction played a

dominant role, while the reduction in the effective pore radius of the membranes by the foulants was significant. In the cases where THM fluxes in Aquaporin increased after alginate fouling, the enhanced concentration polarization may play a role, because the alginate fouling layer is known to feature a tight cross-linking structure [74]. Considering two exampled THMs (TCM and TBM), both exhibited increased interaction with Aquaporin surface after fouling (Table SI-6). However, TCM fluxes decreased after fouling, while TBM fluxes increased, suggesting that the reduction in the effective pore size played a major role for the smaller TCM.

3.4. Comparison of DBP Rejection and Permeance between FO and RO

Figure SI-13 compares the rejection of halogenated DBPs by FO (Aquaporin, this study) and RO membranes (ESPA2 [19]). ESPA2 is a low-pressure brackish water RO membrane that has been used in wastewater recycling facilities [75]. The rejection of halogenated DBPs by Aquaporin in FO is higher than or comparable with that by ESPA2 in RO.

Table 4 compares the rejection and permeance of NDMA in FO determined in this study with those reported for RO in previous studies. NDMA rejection varied in both FO and RO with membrane types, feed waters, and water fluxes, but it was lower in FO (4–31%) than in RO (13–82%). However, NDMA rejection by Aquaporin in FO (16%–34%) was comparable with that in RO (13%–25% [24, 27]) operated at low water fluxes (< 10 L/(m^2·h)). High NDMA rejection in RO (54%–70%) was only observed when water flux exceeded 40 L/(m^2·h) [24, 26, 32]. NDMA permeance in the RO studies were calculated based on water flux, rejection, solution viscosity, membrane dimension, and cross flow rate when available, and were compared with the NDMA permeance in FO obtained from this study. Aquaporin membrane exhibited lower NDMA permeance (0.96 μm/s) than the majority of the low pressure brackish water RO membranes (1.18–

8.28 μm/s) except BW30. ESPAB and SWC5 featured lower NDMA permeance (0.77 μm/s and 0.87 μm/s) than Aquaporin membrane, as expected from their particular design for seawater treatment and boron rejection, respectively.

Table 4. Comparison of NDMA rejection by RO and FO membranes.

Membrane			Study scale	Membrane fouling	Feed concentration C_F (μg/L)	Water flux J_v (L/(m2·h))	Rejection R (%)	Permeance B[b] (μm/s)	Reference
RO	Low pressure brackish water membrane	ESPA2	Bench	Clean	0.25	20	34	6.79	[25]
				Clean	0.05	5	13	8.28	[27]
				Tertiary effluent	0.25	20	73	N.A.	
				Alginate	0.25	20	36	N.A.	[25]
				BSA	0.25	20	32	N.A.	
			Plant	N.A.[a]	0.018-0.057	20.4	24-56	N.A.	[29]
		ESPA3	Bench	Clean	200	57	54	1.18	[26]
				Alginate	200	48	37	N.A.	
		TFC-HR	Bench	Clean	0.25	60	63	2.44	[24]
				Clean	0.25	5	25	3.71	
			Pilot	N.A.	0.25	20	31	N.A.	[30]
		RE-BE	Bench	Clean	880	46.6	65	2.34	[32]
		BW30	Bench	Clean	200	57	61	0.89	[26]
		CTA hollow fiber	Bench	Clean	0.25	3.1	25	N.A.	[31]
	Low fouling brackish water membrane	LFC3	Bench	Clean	0.05	20	37	5.95	[27]
				Clean	200	61	70	0.53	[26]
	Brackish water membrane for boron rejection	ESPAB	Bench	Clean	0.25	20	82	0.77	[25]
	Seawater membrane	SWC5	Bench	Clean	0.25	20	80	0.87	[24]
FO	CTA FO membrane	CTA	Bench	Clean	10	6	4	1.57	This study
				Alginate	10	3.6	20	N.A.	
				BSA	10	3.2	3	N.A.	
	Thin film composite membrane embedded with aquaporin	Aquaporin	Bench	Clean	10	8.1	31	0.96	This study
				Alginate	10	5.7	34	N.A.	
				BSA	10	3.8	16	N.A.	

a N.A.: Not available.

b NDMA permeance was calculated based on water flux, rejection, setup dimensions, and cross flow rate from each RO paper.

217

Published RO studies only evaluated the influence of fouling on nitrosamine and THM rejection, but not on HAN and HK rejection. For NDMA, conflicting results were reported. One study reported a 17% drop in NDMA rejection after the ESPA3 membrane was fouled by alginate (15% water flux decline) [26], while another study reported an increase in NDMA rejection from 34% to 73% after the ESPA2 membrane was fouled by wastewater effluent (25% water flux decline) [25]. We observed that the FO rejection of NDMA increased after alginate fouling of CTA membrane, decreased after BSA fouling of Aquaporin membranes, and was not affected by BSA fouling of CTA or alginate fouling of Aquaporin. The rejection of THMs in RO by XLE membrane increased after membrane fouling by wastewater [20], in contrast to the decrease in THM rejection in FO after Aquaporin and CTA were fouled by alginate or BSA.

4. Conclusion

This study evaluated the rejection of four groups of neutral DBPs (nitrosamines, THMs, HANs, and HKs) in FO by two commercial FO membranes (Aquaporin and CTA). Aquaporin exhibited better rejection performance for all DBPs than CTA. The rejection of high priority DBPs (NDMA and HANs) by Aquaporin was 31% and 48%–76%, respectively. The DBP rejection positively correlates with molecular size across different DBP groups, while the correlation between the DBP rejection and hydrophobicity is not significant. DBP flux through Aquaporin was lower than that through CTA. The rejection of DBPs by Aquaporin in FO determined in this study is comparable with that in RO reported in the literature.

This study is one of the first attempts to determine the effects of fouling on the transport and rejection of neutral DBPs that are relevant to wastewater recycling in FO. Organic fouling decreased the rejection and flux of most DBPs. After fouling, Aquaporin remained more effective

in rejecting DBPs than CTA, despite the fact that fouling negatively impacted Aquaporin performance to a greater extent.

We attempted to use a solution-diffusion model to predict DBP rejection, which incorporates size exclusion, DBP-membrane interaction, and DBP diffusion within the membrane. For the two selected DBPs (TCM and TBM), the model overestimated the transmembrane fluxes for both Aquaporin and CTA membranes by a factor of 1.6–1.9 and 2.4–3.5, respectively. Future research is needed to verify whether the model accuracy can be improved by considering reverse salt flux in the FO transport model.

Acknowledgment

This work is partially supported by the funding provided by the NYS Pollution Prevention Institute through a grant from the New York State Department of Environmental Conservation (GC-2015-01-19) and the National Science Foundation CBET Division (1652412). Any opinions, findings, conclusions or recommendations expressed are those of the authors and do not necessarily reflect the views of the New York State Department of Environmental Conservation.

Appendix A.

Supplementary Information

References

[1] T.Y. Cath, A.E. Childress, M. Elimelech, Forward osmosis: Principles, applications, and recent developments, J Membr. Sci. 281 (2006) 70-87.
[2] K. Lutchmiah, A.R.D. Verliefde, K. Roest, L.C. Rietveld, E.R. Cornelissen, Forward osmosis for application in wastewater treatment: A review, Water Res. 58 (2014) 179-197.
[3] R. Valladares Linares, Z. Li, S. Sarp, S.S. Bucs, G. Amy, J.S. Vrouwenvelder, Forward osmosis niches in seawater desalination and wastewater reuse, Water Res. 66 (2014) 122-139.
[4] M. Qin, Z. He, Self-supplied ammonium bicarbonate draw solute for achieving wastewater treatment and recovery in a microbial electrolysis cell-forward osmosis-coupled system, Environ. Sci. Technol. Lett. 1 (2014) 437-441.
[5] V. Yangali-Quintanilla, Z. Li, R. Valladares, Q. Li, G. Amy, Indirect desalination of Red Sea water with forward osmosis and low pressure reverse osmosis for water reuse, Desalination 280 (2011) 160-166.
[6] Y. Zhang, L. Pinoy, B. Meesschaert, B. Van der Bruggen, A natural driven membrane process for brackish and wastewater treatment: photovoltaic powered ED and FO hybrid system, Environ. Sci. Technol. 47 (2013) 10548-10555.
[7] D.L. Shaffer, N.Y. Yip, J. Gilron, M. Elimelech, Seawater desalination for agriculture by integrated forward and reverse osmosis: Improved product water quality for potentially less energy, J. Membr. Sci. 415-416 (2012) 1-8.
[8] B. Mi, M. Elimelech, Organic fouling of forward osmosis membranes: Fouling reversibility and cleaning without chemical reagents, J. Membr. Sci. 348 (2010) 337-345.
[9] Y. Jang, H. Cho, Y. Shin, Y. Choi, S. Lee, J. Koo, Comparison of fouling propensity and physical cleaning effect in forward osmosis, reverse osmosis, and membrane distillation, Desalin. Water Treat. 57 (2016) 24532-24541.
[10] A. Simon, L.D. Nghiem, P. Le-Clech, S.J. Khan, J.E. Drewes, Effects of membrane degradation on the removal of pharmaceutically active compounds (PhACs) by NF/RO filtration processes, J. Membr. Sci. 340 (2009) 16-25.
[11] A.M. Comerton, R.C. Andrews, D.M. Bagley, C. Hao, The rejection of endocrine disrupting and pharmaceutically active compounds by NF and RO membranes as a function of compound and water matrix properties, J. Membr. Sci. 313 (2008) 323-335.
[12] K. Kimura, S. Toshima, G. Amy, Y. Watanabe, Rejection of neutral endocrine disrupting compounds (EDCs) and pharmaceutical active compounds (PhACs) by RO membranes, J. Membr. Sci. 245 (2004) 71-78.
[13] H. Ozaki, K. Fukami, N. Ikejima, S. Matsui, Y. Shimizu, R.R. Giri, S. Taniguchi, R. Takanami, Rejection of pharmaceuticals and personal care products (PPCPs) and endocrine disrupting chemicals (EDCs) by low pressure reverse osmosis membranes, Water Sci. Technol. 58 (2008) 73.
[14] J. Radjenović, M. Petrović, F. Ventura, D. Barceló, Rejection of pharmaceuticals in nanofiltration and reverse osmosis membrane drinking water treatment, Water Res. 42 (2008) 3601-3610.
[15] J.H. Al-Rifai, H. Khabbaz, A.I. Schäfer, Removal of pharmaceuticals and endocrine disrupting compounds in a water recycling process using reverse osmosis systems, Sep. Purif. Technol. 77 (2011) 60-67.
[16] D. Dolar, T. Ignjatić Zokić, K. Košutić, D. Ašperger, D. Mutavdžić Pavlović, RO/NF membrane treatment of veterinary pharmaceutical wastewater: comparison of results obtained on a laboratory and a pilot scale, Environ. Sci. Pollut. Res. 19 (2012) 1033-1042.

[17] T. Zeng, M.J. Plewa, W.A. Mitch, *N*-Nitrosamines and halogenated disinfection byproducts in US Full Advanced Treatment trains for potable reuse, Water Res. 101 (2016) 176-186.
[18] K. Kimura, G. Amy, J.E. Drewes, T. Heberer, T.-U. Kim, Y. Watanabe, Rejection of organic micropollutants (disinfection by-products, endocrine disrupting compounds, and pharmaceutically active compounds) by NF/RO membranes, J. Membr. Sci. 227 (2003) 113-121.
[19] K. Doederer, M.J. Farré, M. Pidou, H.S. Weinberg, W. Gernjak, Rejection of disinfection by-products by RO and NF membranes: Influence of solute properties and operational parameters, J. Membr. Sci. 467 (2014) 195-205.
[20] P. Xu, J.E. Drewes, T.-U. Kim, C. Bellona, G. Amy, Effect of membrane fouling on transport of organic contaminants in NF/RO membrane applications, J. Membr. Sci. 279 (2006) 165-175.
[21] P. Xu, J.E. Drewes, C. Bellona, G. Amy, T.-U. Kim, M. Adam, T. Heberer, Rejection of emerging organic micropollutants in nanofiltration–reverse osmosis membrane applications, Water Environ. Res. 77 (2005) 40-48.
[22] E. Agus, D.L. Sedlak, Formation and fate of chlorination by-products in reverse osmosis desalination systems, Water Res. 44 (2010) 1616-1626.
[23] U.S. EPA, National Primary Drinking Water Regulations, in, U.S. Government Printing Office, Washington, DC, 2010.
[24] T. Fujioka, L.D. Nghiem, S.J. Khan, J.A. McDonald, Y. Poussade, J.E. Drewes, Effects of feed solution characteristics on the rejection of *N*-nitrosamines by reverse osmosis membranes, J. Membr. Sci. 409-410 (2012) 66-74.
[25] T. Fujioka, S.J. Khan, J.A. McDonald, R.K. Henderson, Y. Poussade, J.E. Drewes, L.D. Nghiem, Effects of membrane fouling on *N*-nitrosamine rejection by nanofiltration and reverse osmosis membranes, J. Membr. Sci. 427 (2013) 311-319.
[26] E. Steinledarling, M. Zedda, M. Plumlee, H. Ridgway, M. Reinhard, Evaluating the impacts of membrane type, coating, fouling, chemical properties and water chemistry on reverse osmosis rejection of seven nitrosoalklyamines, including NDMA, Water Res. 41 (2007) 3959-3967.
[27] T. Fujioka, S.J. Khan, J.A. McDonald, A. Roux, Y. Poussade, J.E. Drewes, L.D. Nghiem, *N*-nitrosamine rejection by nanofiltration and reverse osmosis membranes: The importance of membrane characteristics, Desalination 316 (2013) 67-75.
[28] T. Fujioka, S.J. Khan, J.A. McDonald, A. Roux, Y. Poussade, J.E. Drewes, L.D. Nghiem, *N*-nitrosamine rejection by reverse osmosis membranes: A full-scale study, Water Res. 47 (2013) 6141-6148.
[29] M.H. Plumlee, M. López-Mesas, A. Heidlberger, K.P. Ishida, M. Reinhard, *N*-nitrosodimethylamine (NDMA) removal by reverse osmosis and UV treatment and analysis via LC–MS/MS, Water Res. 42 (2008) 347-355.
[30] T. Fujioka, K.L. Tu, S.J. Khan, J.A. McDonald, A. Roux, Y. Poussade, J.E. Drewes, L.D. Nghiem, Rejection of small solutes by reverse osmosis membranes for water reuse applications: A pilot-scale study, Desalination 350 (2014) 28-34.
[31] T. Fujioka, S.J. Khan, J.A. McDonald, L.D. Nghiem, Rejection of trace organic chemicals by a hollow fibre cellulose triacetate reverse osmosis membrane, Desalination 368 (2015) 69-75.
[32] Y. Miyashita, S.H. Park, H. Hyung, C.H. Huang, J.H. Kim, Removal of *N*-nitrosamines and their precursors by nanofiltration and reverse osmosis membranes, J. Environ. Eng. 135 (2009) 788-795.
[33] U.S. EPA, IRIS Toxicological and Summary Documents, in, U.S. Environmental Protection Agency, Washington, DC.

[34] N. Dai, T. Zeng, W.A. Mitch, Predicting *N*-nitrosamines: *N*-nitrosodiethanolamine as a significant component of total *N*-nitrosamines in recycled wastewater, Environ. Sci. Tech. Let. 2 (2015) 54-58.
[35] Y. Du, X.T. Lv, Q.Y. Wu, D.Y. Zhang, Y.T. Zhou, L. Peng, H.Y. Hu, Formation and control of disinfection byproducts and toxicity during reclaimed water chlorination: A review, J. Environ. Sci. 58 (2017) 51-63.
[36] T. Fujioka, S.J. Khan, Y. Poussade, J.E. Drewes, L.D. Nghiem, *N*-nitrosamine removal by reverse osmosis for indirect potable water reuse – A critical review based on observations from laboratory-, pilot- and full-scale studies, Sep. Purif. Technol. 98 (2012) 503-515.
[37] S.W. Krasner, P. Westerhoff, B. Chen, B.E. Rittmann, G. Amy, Occurrence of disinfection byproducts in United States wastewater treatment plant effluents, Environ. Sci. Technol. 43 (2009) 8320-8325.
[38] National Research Council, Water Reuse: Expanding the Nation's Water Supply through Reuse of Municipal Wastewater, in, Washington, DC, 2012.
[39] S. Richardson, M. Plewa, E. Wagner, R. Schoeny, D. Demarini, Occurrence, genotoxicity, and carcinogenicity of regulated and emerging disinfection by-products in drinking water: A review and roadmap for research, Mutat. Res. Rev. Mutat. Res. 636 (2007) 178-242.
[40] A.A. Alturki, J.A. McDonald, S.J. Khan, W.E. Price, L.D. Nghiem, M. Elimelech, Removal of trace organic contaminants by the forward osmosis process, Sep. Purif. Technol. 103 (2013) 258-266.
[41] B.D. Coday, B.G.M. Yaffe, P. Xu, T.Y. Cath, Rejection of trace organic compounds by forward osmosis membranes: A literature review, Environ. Sci. Technol. 48 (2014) 3612-3624.
[42] R. Valladares Linares, V. Yangali-Quintanilla, Z. Li, G. Amy, Rejection of micropollutants by clean and fouled forward osmosis membrane, Water Res. 45 (2011) 6737-6744.
[43] M. Xie, L.D. Nghiem, W.E. Price, M. Elimelech, Relating rejection of trace organic contaminants to membrane properties in forward osmosis: Measurements, modelling and implications, Water Res. 49 (2014) 265-274.
[44] Y.L. Lin, C.H. Lee, Elucidating the rejection mechanisms of PPCPs by nanofiltration and reverse osmosis membranes, Ind Eng Chem Res, 53 (2014) 6798-6806.
[45] H.T. Madsen, N. Bajraktari, C. Helix-Nielsen, B. Van der Bruggen, E.G. Sogaard, Use of biomimetic forward osmosis membrane for trace organics removal, J. Membr. Sci. 476 (2015) 469-474.
[46] M. Xie, W. Luo, H. Guo, L.D. Nghiem, C.Y. Tang, S.R. Gray, Trace organic contaminant rejection by aquaporin forward osmosis membrane: Transport mechanisms and membrane stability, Water Res. 132 (2018) 90-98.
[47] S. Engelhardt, A. Sadek, S. Duirk, Rejection of trace organic water contaminants by an Aquaporin-based biomimetic hollow fiber membrane, Sep. Purif. Technol. 197 (2018) 170-177.
[48] S. Zhao, K. Huang, H. Lin, Impregnated membranes for water purification using forward osmosis, Ind. Eng. Chem. Res. 54 (2015) 12354-12366.
[49] H. Lin, S.M. Thompson, A. Serbanescu-Martin, J.G. Wijmans, K.D. Amo, K.A. Lokhandwala, T.C. Merkel, Dehydration of natural gas using membranes. Part I: Composite membranes, J. Membr. Sci. 413-414 (2012) 70-81.
[50] K. Yu, M.C. Reichard, N. Dai, Nitrosamine formation in the desorber of tertiary alkanolamine-based carbon dioxide capture systems, Ind. Eng. Chem. Res. 55 (2016) 2604-2614.
[51] C.J. van Oss, Development and applications of the interfacial tension between water and organic or biological surfaces, Colloids Surf., B 54 (2007) 2-9.

[52] A.R.D. Verliefde, E.R. Cornelissen, S.G.J. Heijman, E.M.V. Hoek, G.L. Amy, B.V.d. Bruggen, J.C. van Dijk, Influence of solute−membrane affinity on rejection of uncharged organic solutes by nanofiltration membranes, Environ. Sci. Technol. 43 (2009) 2400-2406.
[53] S. Botton, A.R.D. Verliefde, N.T. Quach, E.R. Cornelissen, Influence of biofouling on pharmaceuticals rejection in NF membrane filtration, Water Res. 46 (2012) 5848-5860.
[54] F.X. Kong, H.W. Yang, Y.Q. Wu, X.M. Wang, Y.F. Xie, Rejection of pharmaceuticals during forward osmosis and prediction by using the solution–diffusion model, J. Membr. Sci. 476 (2015) 410-420.
[55] Y. Yu, D.A. Reckhow, Kinetic Analysis of Haloacetonitrile Stability in Drinking Waters, Environ. Sci. Technol. 49 (2015) 11028-11036.
[56] P.C. Chiang, E.E. Chang, C.C. Chuang, C.H. Liang, C.P. Huang, Evaluating and elucidating the formation of nitrogen-contained disinfection by-products during pre-ozonation and chlorination, Chemosphere 80 (2010) 327-333.
[57] M.J. Plewa, E.D. Wagner, Mammalian cell cytotoxicity and genotoxicity of disinfection by-product, Water Research Foundation, Denver, CO, 2009.
[58] National Research Council, Use of Reclaimed Water and Sludge in Food Crop Production, The National Academies Press, Washington, DC, 1996.
[59] L.D. Nghiem, A.I. Schafer, M. Elimelech, Removal of natural hormones by nanofiltration membranes: Measurement, modeling, and mechanisms, Environ. Sci. Technol. 38 (2004) 1888-1896.
[60] L.D. Nghiem, A.I. Schafer, M. Elimelech, Pharmaceutical retention mechanisms by nanofiltration membranes, Environ. Sci. Technol. 39 (2005) 7698-7705.
[61] T. Dey, Nanotechnology for Water Purification, BrownWalker Press, Boca Raton, Florida, 2012.
[62] J. Radjenovic, M. Petrovic, F. Ventura, D. Barcelo, Rejection of pharmaceuticals in nanofiltration and reverse osmosis membrane drinking water treatment, Water Res. 42 (2008) 3601-3610.
[63] A.I. Schafer, L.D. Nghiem, T.D. Waite, Removal of the natural hormone estrone from aqueous solutions using nanofiltration and reverse osmosis, Environ. Sci. Technol. 37 (2003) 182-188.
[64] J. Wang, Y. Mo, S. Mahendra, E.M.V. Hoek, Effects of water chemistry on structure and performance of polyamide composite membranes, J. Membr. Sci. 452 (2014) 415-425.
[65] J.W. Wang, D.S. Dlamini, A.K. Mishra, M.T.M. Pendergast, M.C.Y. Wong, B.B. Mamba, V. Freger, A.R.D. Verliefde, E.M.V. Hoek, A critical review of transport through osmotic membranes, J. Membr. Sci. 454 (2014) 516-537.
[66] L.L. Xia, M.F. Andersen, C. Helix-Nielsen, J.R. McCutcheon, Novel commercial aquaporin flat-sheet membrane for forward Osmosis, Ind. Eng. Chem. Res. 56 (2017) 11919-11925.
[67] M. Xie, L.D. Nghiem, W.E. Price, M. Elimelech, Comparison of the removal of hydrophobic trace organic contaminants by forward osmosis and reverse osmosis, Water Res. 46 (2012) 2683-2692.
[68] S. Bhattacharjee, A. Sharma, P.K. Bhattacharya, Estimation and influence of long range solute. Membrane interactions in ultrafiltration, Ind. Eng. Chem. Res. 35 (1996) 3108-3121.
[69] W.M. Deen, Hindered transport of large molecules in liquid-filled pores, Aiche J. 33 (1987) 1409-1425.
[70] C. van Oss, Interfacial Forces in Aqueous Media, Second Edition, CRC Press, 2006.

[71] B. Janczuk, E. Chibowski, J.M. Bruque, M.L. Kerkeb, F.G. Caballero, On the Consistency of Surface Free Energy Components as Calculated from Contact Angles of Different Liquids: An Application to the Cholesterol Surface, J. Colloid Interface Sci. 159 (1993) 421-428.
[72] J.N. Israelachvili, Intermolecular and Surface Forces, 3rd ed., Academic Press, Burlington, MA, 2011.
[73] E.M.V. Hoek, M. Elimelech, Cake-enhanced concentration polarization: A new fouling mechanism for salt-rejecting membranes, Environ. Sci. Technol. 37 (2003) 5581-5588.
[74] B. Mi, M. Elimelech, Chemical and physical aspects of organic fouling of forward osmosis membranes, J. Membr. Sci. 320 (2008) 292-302.
[75] C. Bartels, R. Franks, K. Andes, Operational Performance and Optimization of RO Wastewater Treatment Plants, Technical paper, Hydranautics, Oceanside, CA, USA, (2010).

Removal of Disinfection Byproducts in Forward Osmosis for Wastewater Recycling

Supplementary Information

Jiale Xu[1], Thien Ngoc Tran[2], Haiqing Lin[2], Ning Dai[1*]

[1]Department of Civil, Structural and Environmental Engineering
University at Buffalo, The State University of New York, Buffalo, NY, 14260

[2]Department of Chemical and Biological Engineering
University at Buffalo, The State University of New York, Buffalo, NY, 14260

[*]Corresponding author: Post address: 231 Jarvis Hall, Buffalo, NY 14260
Phone: (716) 645-4015; Fax: (716) 645-3667
Email: ningdai@buffalo.edu

3 Texts, 6 Tables, and 13 Figures

Text SI-1. Calculation of water and DBP fluxes, DBP rejection and DBP permeability.

For all experiments, water flux was calculated as

$$J_{v,t+0.5\Delta t} = \frac{V_{D,t+\Delta t} - V'_{D,t}}{A_M \Delta t} \quad \text{(S1)}$$

where $J_{v,\,t+0.5\Delta t}$ (L/(m^2·h)) is the average water flux within each sampling time interval; $V'_{D,t}$ (L) and $V_{D,t+\Delta t}$ (L) are the volumes of draw solution after sampling at time t and before the subsequent sampling at $t+\Delta t$, respectively; A_M (m^2) is the effective membrane area; and Δt (h) is the time interval between the two sampling. The average DBP flux through membrane was calculated by

$$J_{DBP,t+0.5\Delta t} = \frac{C_{D,t+\Delta t}V_{D,t+\Delta t} - C_{D,t}V'_{D,t}}{A_M \Delta t} \quad \text{(S2)}$$

where $J_{DBP,\,t+0.5\Delta t}$ (μg/(m^2·h)) is the average DBP flux within each sampling time interval; C_D (μg/L) is DBP concentration in the draw solution, at time t or $t+\Delta t$ as specified by the subscript. The average DBP rejection within each time interval was calculated using equation S3.

$$R_{t+0.5\Delta t} = \left[1 - \frac{2J_{DBP,t+0.5\Delta t}}{J_{v,t+0.5\Delta t}\left(C_{F,t+\Delta t} + C_{F,t}\right)}\right] \times 100\% \quad \text{(S3)}$$

where $R_{t+0.5\Delta t}$ (%) is the average DBP rejection between t and $t+\Delta t$; and C_F (μg/L) is the DBP concentrations in the feed solution, at time t or $t+\Delta t$ as specified by the subscript.

DBP permeability coefficient B_{DBP} (m/s) was calculated by the following equation:

$$B_{DBP} = \frac{J_{DBP}}{(\beta C_{F,t} - C_{D,t})_{average}} \quad \text{(S4)}$$

where β is the concentration polarization factor calculated as described in Text SI-2; J_{DBP} (μg/(m^2·h)) is the stabilized DBP flux (i.e., the average of DBP fluxes measured after stabilization were established); $C_{F,t}$ and $C_{D,t}$ are the DBP concentration in feed and draw solutions at time t, respectively, after DBP rejection was stabilized. Concentration polarization factor is a function of cross-flow rate, solution viscosity, and water flux.

Text SI-2. Concentration polarization calculation.

Concentration polarization of DBPs occurs near membrane surface on the feed side. The extent of concentration polarization is described by the ratio between DBP concentration at the membrane surface (C_M (M)) and that in the bulk phase of the feed solution (C_F (M)).

$$\beta = \frac{C_M}{C_F} \tag{S5}$$

where β (dimensionless) is the concentration polarization factor. Because the transport of DBP from the bulk solution to membrane surface in FO is similar to that of salt in RO, equations derived for the latter apply.

$$\frac{C_M - C_D}{C_F - C_D} = \exp(J_v / k_{CP}) \tag{S6}$$

where C_D (M) is the DBP concentration in the bulk phase of the draw solution; J_v (m/s) is the water flux through membrane; and k_{CP} (m/s) is the concentration polarization mass transfer coefficient. For flat-sheet membrane cells [1], k_{CP} can be calculated by the equations of

$$k_{CP} = 0.664 \frac{D_L}{d_H} (\mathrm{Re})^{0.5} (\mathrm{Sc})^{0.33} (\frac{d_H}{L})^{0.5} \tag{S7}$$

$$\mathrm{Re} = \frac{\rho v d_H}{\mu} \tag{S8}$$

$$\mathrm{Sc} = \frac{\mu}{\rho D_L} \tag{S9}$$

where D_L is the diffusion coefficient of DBP in water; Re (dimensionless) is the Reynolds number; Sc (dimensionless) is the Schmidt number; d_H (m) is the channel depth of membrane cell; L (m) is the cell length of membrane cell; ρ (kg/m^3) is water density; v (m/s) is the crossflow velocity; μ (Pa·s) is the dynamic viscosity of solution. In this study, dynamic viscosity of water was used, because the solution has a very low concentration of DBPs (10 or 20 μg/L).

Text SI-3. Membrane pore size determination.

A procedure reported by previous studies was adopted [2, 3]. Glycerol and ethyl acetate were used as the reference organic solutes to estimate the effective pore radius r_p and the ratio of the membrane thickness to porosity $\Delta x/\varepsilon$. The solutes were individually dissolved in Milli-Q water to obtain a concentration of 400 mg/L (as total organic carbon (TOC)). Membranes were operated in the RO mode in a dead-end cell. The membrane was pre-compacted at 10 bar for one hour with Milli-Q water as feed. The reference organic solution was then used as feed, with a constant pressure of 10 bar. The dead-end cell was operated for 30 minutes before permeate and feed solutions were sample for TOC analysis. $\Delta G_{DBP,M}$ for reference solutes was calculated by applying the surface tension components of glycerol and ethyl acetate [4], and the surface tension components of membranes from Table SI-4 to the equation 5 in the main text. r_s was calculated based on the molecular volume obtained from ACD/Percepta Platform. Diffusion coefficient D was calculated based on Stokes–Einstein equation as shown as equation 6 in the main text and the hindrance factor K_d as shown as equation 7 in the main text. Permeability B was calculated based on equation S4, and β was 1 due to the complete mix of solution by stirring. The membrane average pore radius was determined by solving equation 4 in the main text for glycerol and ethyl acetate with the above known parameters**.**

Table SI-1. Characteristics of the membranes used in this study.

Membranes	Materials	Water flux[a] ($L/(m^2 \cdot h)$)	Reverse NaCl flux[a] ($g/(m^2 \cdot h)$)	NaCl rejection (%)	Zeta potential (mV)	Porosity (%)	Membrane thickness (μm)	Structural parameter (μm)
Aquaporin	Polyamide with aquaporin	8.1	3.5	97.9[b]	–55[c]	N.A.[d]	112[e]	301[f]
CTA	Cellulose acetate	6.0	5.5	94.0[g]	–8[h]	64[i]	90[i]	720[i]

a Draw solution 1 M NaCl; feed concentration: 10 μg/L of nitrosamines and 20 μg/L of halogenated DBPs; temperature 21 ^{o}C;; pH of both solutions 6.5–7.5.
b Feed NaCl concentration 2 g/L; temperature 20 °C; feed pressure 8.62 bar; RO measurement [5].
c 10 mM NaCl at 21 °C pH 6.7 [6].
d N.A.: Not available.
e [7].
f [3].
g Feed NaCl concentration 50 mM; temperature 25 °C; feed pressure 27.2 bar; RO measurement [8].
h 50 mM NaCl at 21 °C pH 6 [9].
i [10].

Table SI-2. Concentration polarization factors for all sixteen DBPs in clean Aquaporin and CTA membrane experiments in this study.

DBP	FO membranes	
	CTA	Aquaporin
NDMA	1.57	1.81
NMEA	0.99	1.98
NPYR	0.98	2.03
NDEA	0.86	2.08
NPIP	0.74	2.11
NDPA	0.56	2.20
NDBA	0.46	2.29
TCM	1.53	1.81
DCBM	1.29	1.90
DBCM	1.10	1.97
TBM	0.92	2.00
DCAN	1.99	1.89
BCAN	1.51	1.94
DBAN	1.03	1.98
1,1-DCP	0.94	2.04
1,1,1-TCP	0.37	2.10

Table SI-3. Correlation tests between FO rejection of DBPs and their MV or log K_{ow} (df[a]=14).

Membranes	MV				log K_{ow}			
	Pearson's r	p-value	Spearman's ρ	p-value	Pearson's r	p-value	Spearman's ρ	p-value
Aquaporin	0.696	0.003	0.920	0.000	0.252	0.347	0.344	0.192
CTA	0.760	0.001	0.862	0.000	0.353	0.179	0.438	0.090

a degree of freedom

Table SI-4. Constants of the Bungay and Brenner correlation to calculate diffusion hindrance factor [11].

a1	a2	a3	a4	a5	a6	a7
-1.22	1.53	22.51	-5.61	-0.34	-1.22	1.65

0

Table SI-5. Diffusion hindrance factor K_d for TCM and TBM.

Membranes	TCM	TBM
Aquaporin	0.0049	0.0015
CTA	0.019	0.011

1

Table SI-6. Surface tension components of membranes and the free energy of interaction between the membrane and TCM or TBM.

Membranes		Surface tension components (mJ/m^2)			Free energy of DBP-membrane interaction, $\Delta G_{DBP,M}$ ($\times 10^{-21}$ J)		DBP-membrane interaction term, $\exp[-(\Delta G_{DBP,M}/kT)]$ (–)	
		γ^{LW}	γ^{+}	γ^{-}	TCM	TBM	TCM	TBM
Aqua-porin	Clean	45.59	0.14	49.46	-3.52	-4.57	2.39	3.09
	Alginate	34.34	0.46	3.20	-7.23	-8.37	5.97	7.92
	BSA	32.78	0.01	1.36	-8.31	-9.53	7.80	10.55
CTA	Clean	32.14	0.00	32.38	-4.80	-5.68	3.28	4.07
	Alginate	36.98	0.29	0.14	-8.51	-9.84	8.20	11.39
	BSA	37.55	0.83	3.29	-7.00	-8.19	5.64	7.57

2

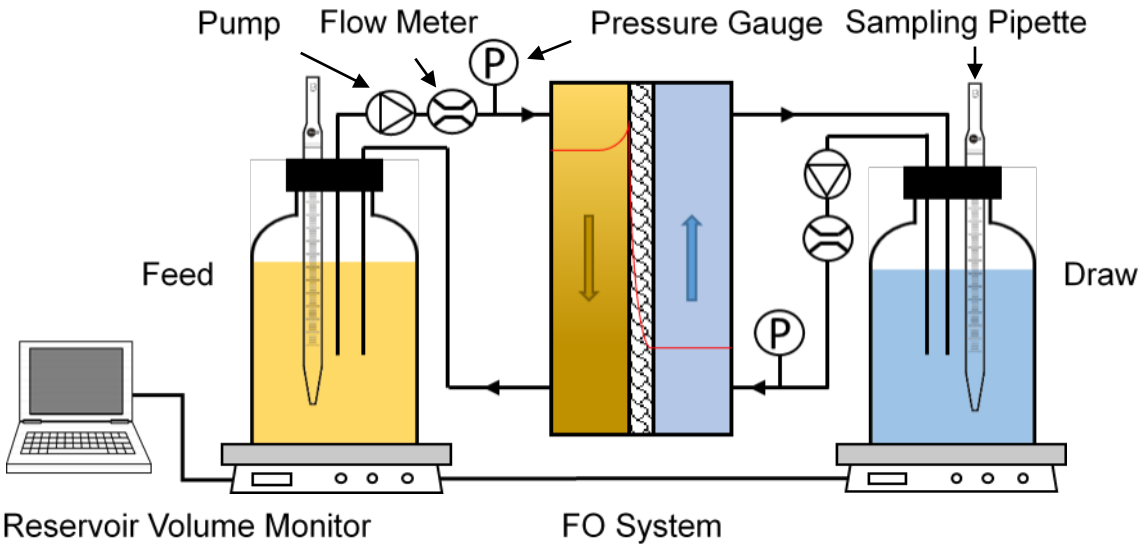

Figure SI-1. Schematic of the bench-scale FO cross-flow system.

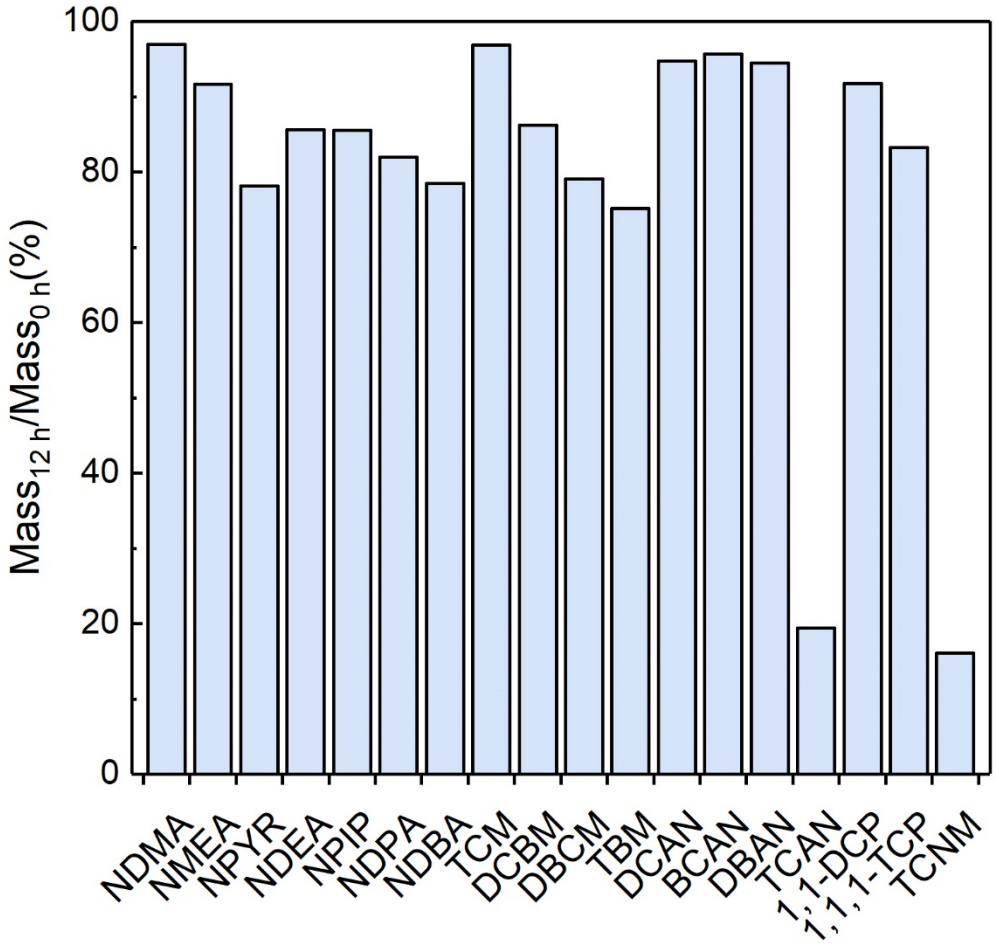

Figure SI-2. Percentage of halogenated DBP mass remaining after 12 h in aqueous solutions at 21 ^{o}C. Halogenated DBP initial concentration 20 µg/L; nitrosamine initial concentration 10 µg/L; solution pH 6.7, unbuffered.

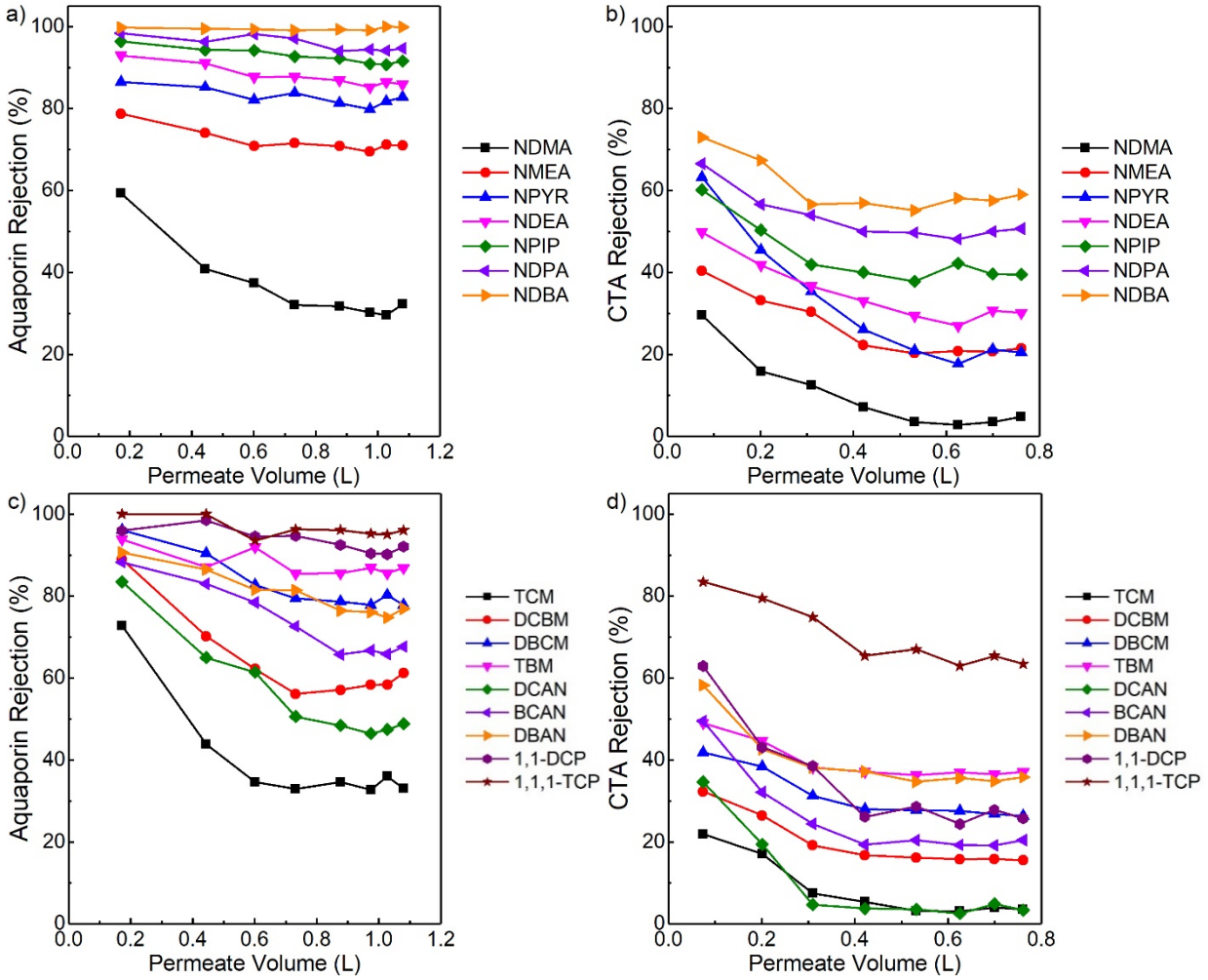

Figure SI-3. Change of (a)–(b) nitrosamine and (c)–(d) halogenated DBP rejection by Aquaporin and CTA as a function of water transport volume. Nitrosamine initial concentration 10 µg/L; halogenated DBP initial concentration 20 µg/L; draw solution 1 M NaCl; temperature 21 ^{o}C; pH 6.5–7.5 for both feed and draw solutions. Water fluxes Aquaporin and CTA membranes were 8.1 and 6.0 L/(m^2·h), respectively. The experimental time was 8 h.

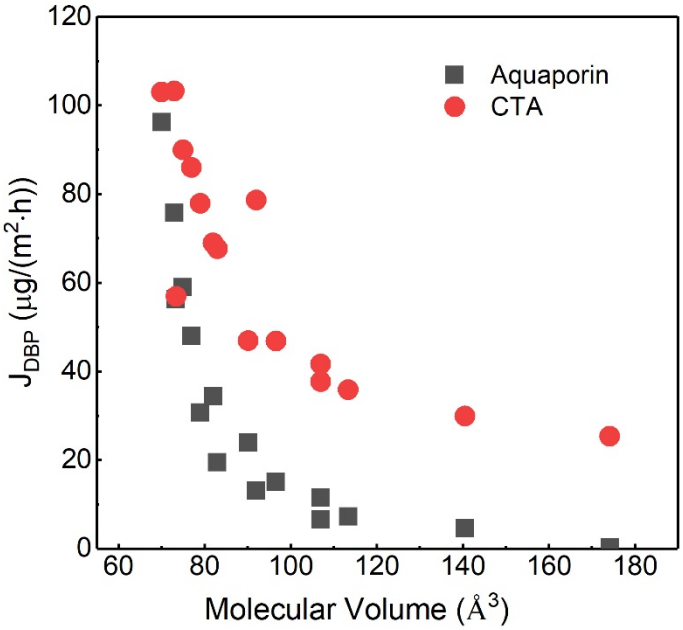

Figure SI-4. DBP fluxes of all sixteen DBPs through Aquaporin and CTA membranes as a function of molecular volume. Water fluxes for Aquaporin and CTA membranes were 8.1 and 6.0 L/(m^2·h), respectively; draw solution 1 M NaCl; nitrosamine concentration 10 µg/L; halogenated DBP concentration 20 µg/L; temperature 21 ^{o}C; solution pH 6.5–7.5.

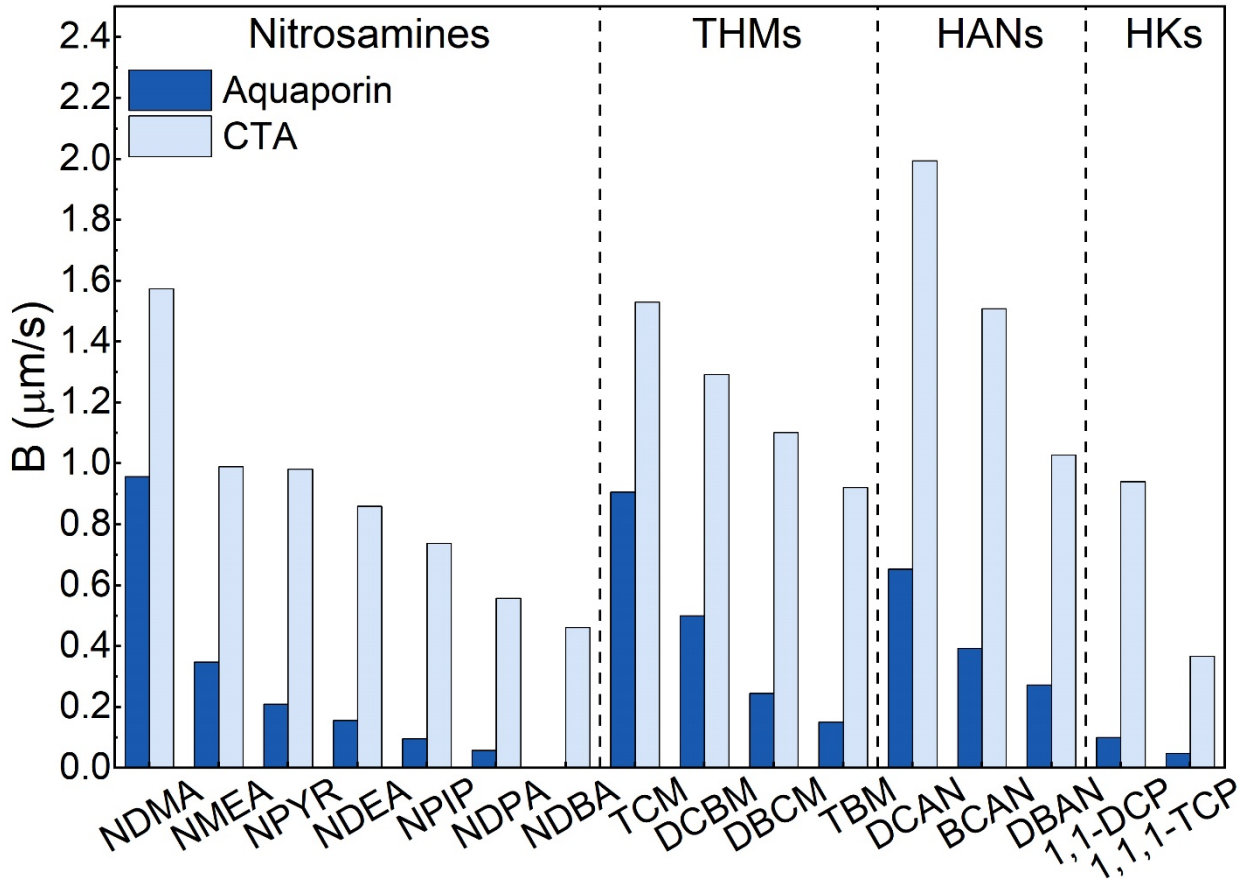

Figure SI-5. DBP permeability coefficient of all sixteen DBPs for Aquaporin and CTA membranes. Water fluxes for Aquaporin and CTA membranes were 8.1 and 6.0 L/(m^2·h), respectively; draw solution 1 M NaCl; nitrosamine concentration 10 μg/L; halogenated DBP concentration 20 μg/L; temperature 21 ^{o}C; solution pH 6.5–7.5.

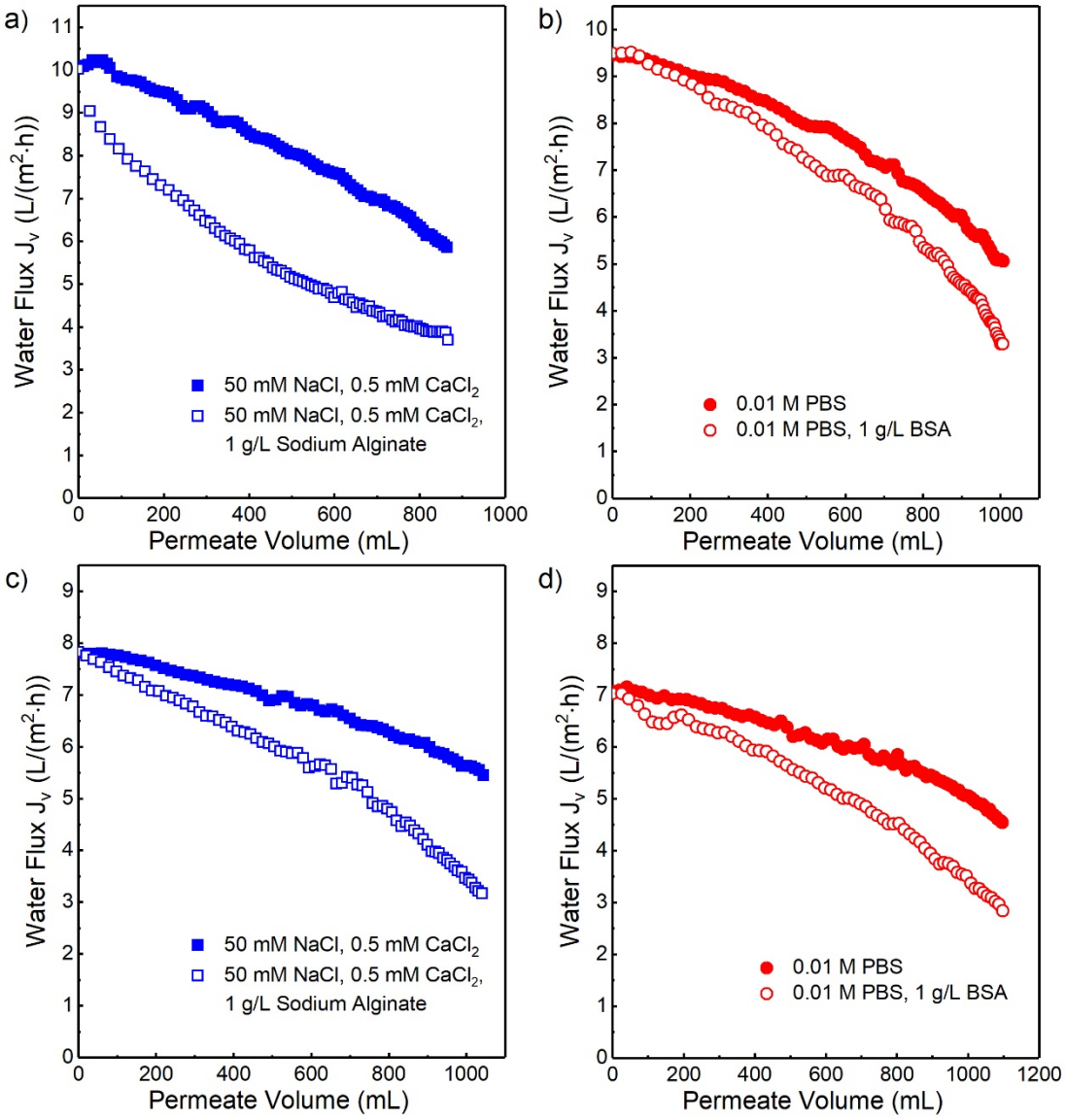

Figure SI-6. Water flux decline of (a)–(b) Aquaporin and (c)–(d) CTA membranes in the presence and absence of foulants. Feed solution condition is shown in legend. Alginate: blue square; BSA: red circle. Draw solution 1.5 M NaCl; pH for all solution 6.5–7.5; temperature 21 ^{o}C. Membranes were exposed to the fouling solutions for 15 hours.

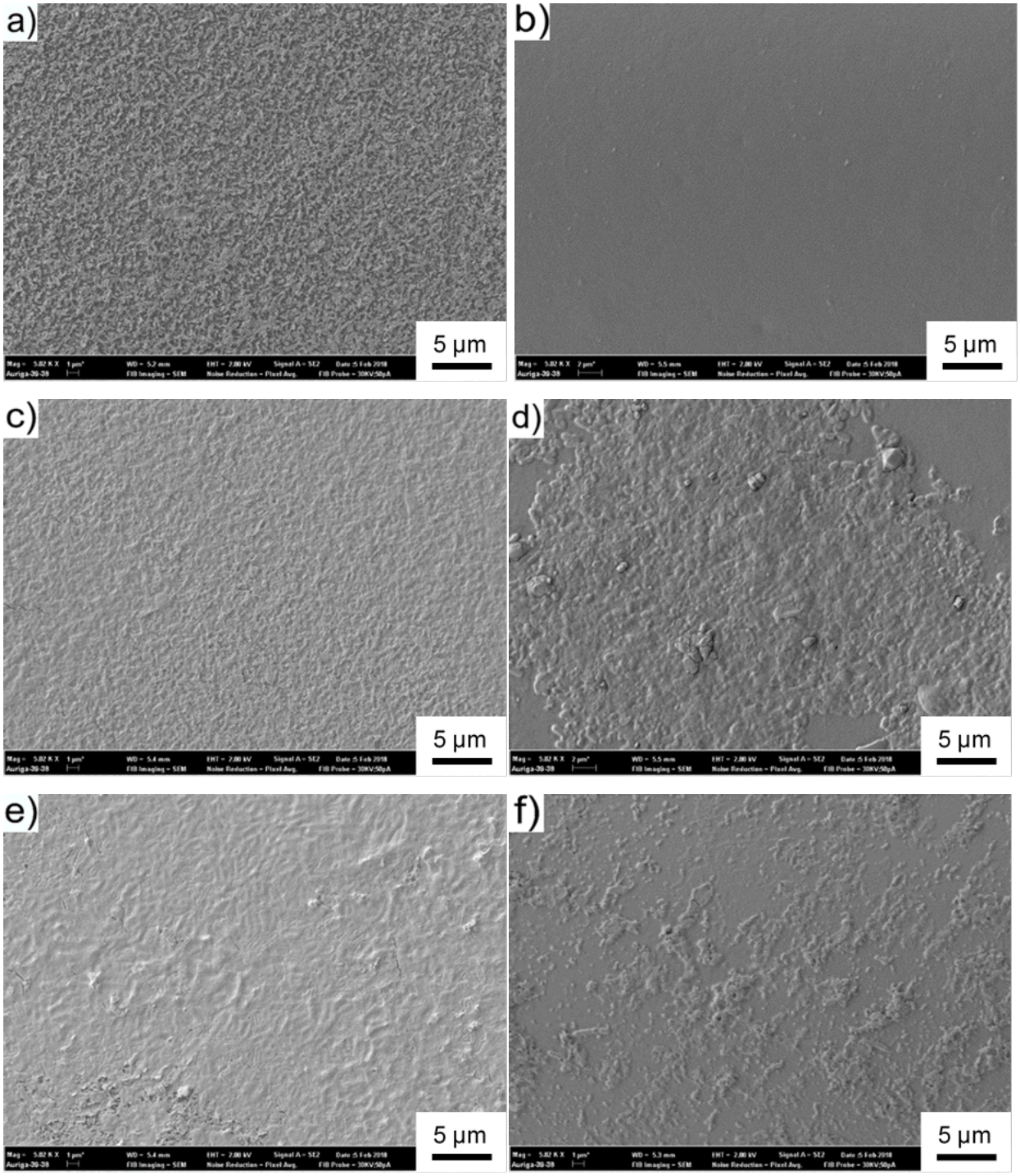

Figure SI-7. Surface SEM images of (a)–(b) clean, (c)–(d) alginate-fouled, and (e)–(f) BSA-fouled membranes (× 5K) for Aquaporin (a, c, and e) and CTA membranes (b, d, and f). Experimental conditions are introduced in Figure SI-5.

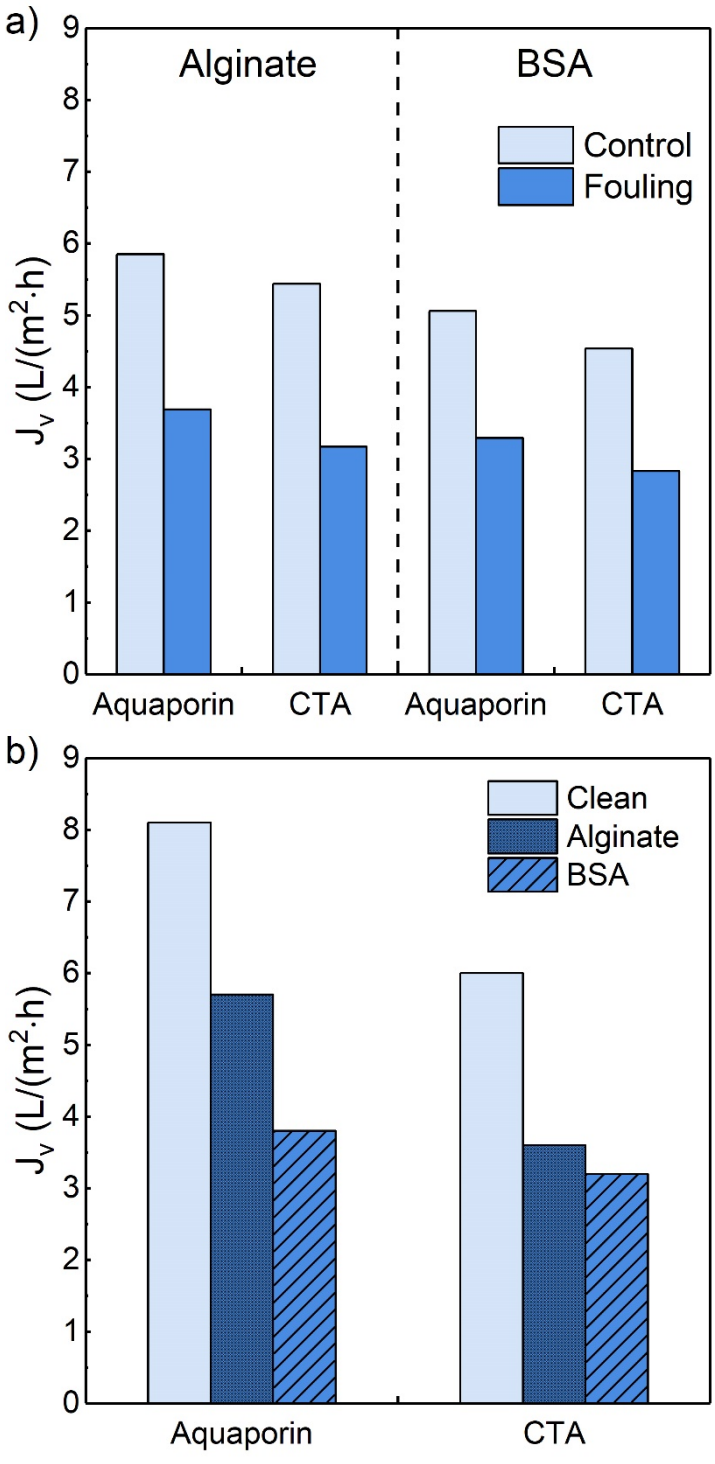

Figure SI-8. (a) Water fluxes after 15 hour fouling generation experiments with and without foulants from Figure SI-5. Experimental conditions are introduced in Figure SI-5. (b) Water fluxes for clean, alginate-fouled, and BSA-fouled membranes in DBP rejection experiments. Draw solution 1 M NaCl; feed solution: DI for clean membrane; 50 mM NaCl, 0.5 mM $CaCl_2$, and 0.2 g/L sodium alginate for alginate-fouled membrane; 0.01 M PBS and 0.2 g/L BSA for BSA-fouled membrane; temperature 21 ^{o}C; pH for both solution 6.5–7.5.

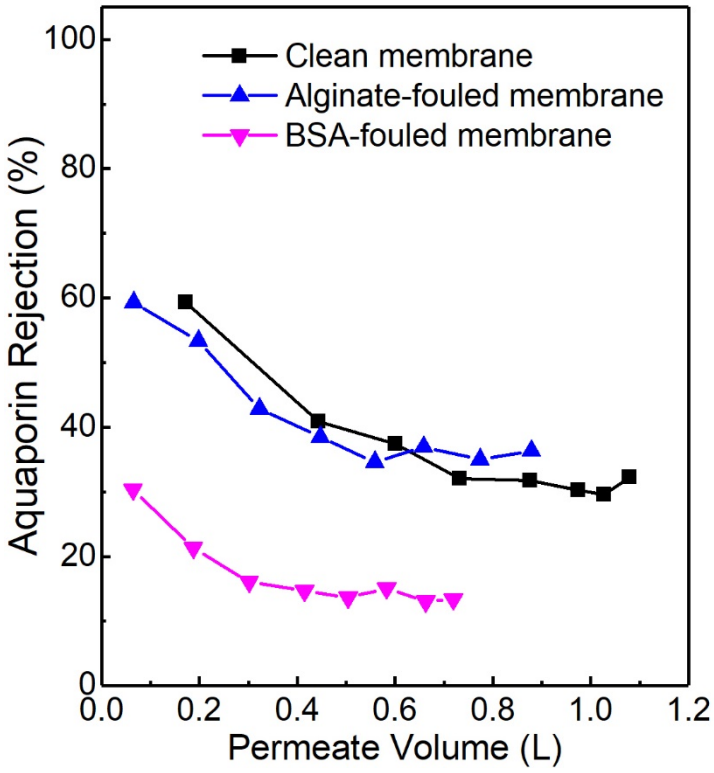

Figure SI-9. The change of NDMA rejection as a function of water transport volume for clean and fouled Aquaporin membranes. NDMA initial concentration 10 μg/L in feed; draw solution 1 M NaCl; temperature 21 ^{o}C; pH 6.5–7.5 for both feed and draw solutions. Water fluxes for clean, alginate-fouled, and BSA-fouled Aquaporin membranes were 8.1, 5.7 and 3.8 L/(m^2·h), respectively. The experimental time was 8 h.

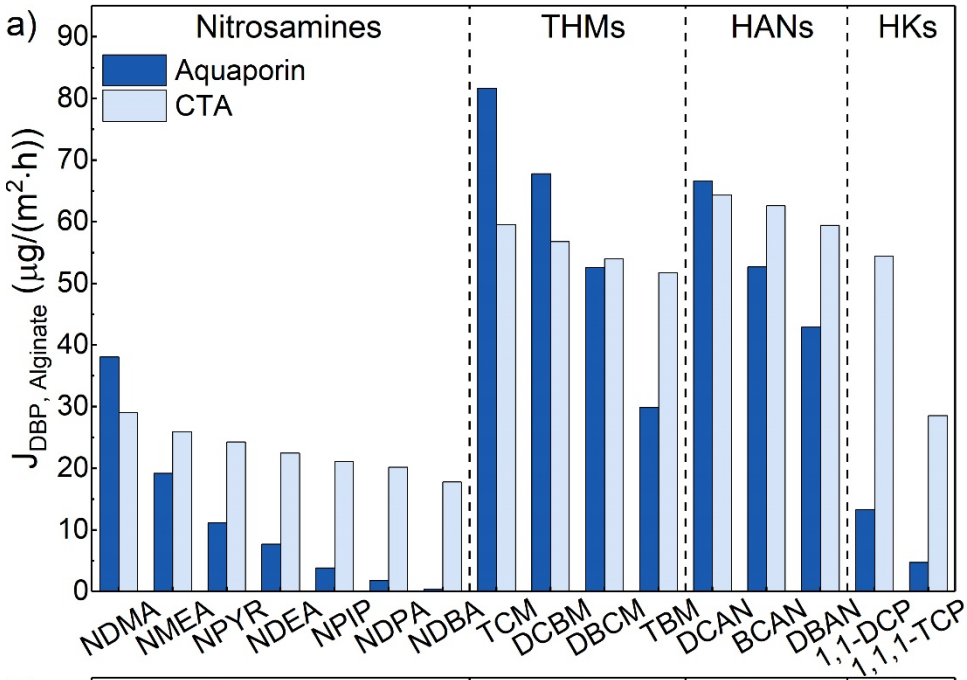
a)
Nitrosamines
THMs
HANs
HKs
Aquaporin
CTA
$J_{DBP, Alginate}$ (μg/(m²·h))
0
10
20
30
40
50
60
70
80
90
NDMA
NMEA
NPYR
NDEA
NPIP
NDPA
NDBA
TCM
DCBM
DBCM
TBM
DCAN
BCAN
DBAN
1,1-DCP
1,1,1-TCP

53

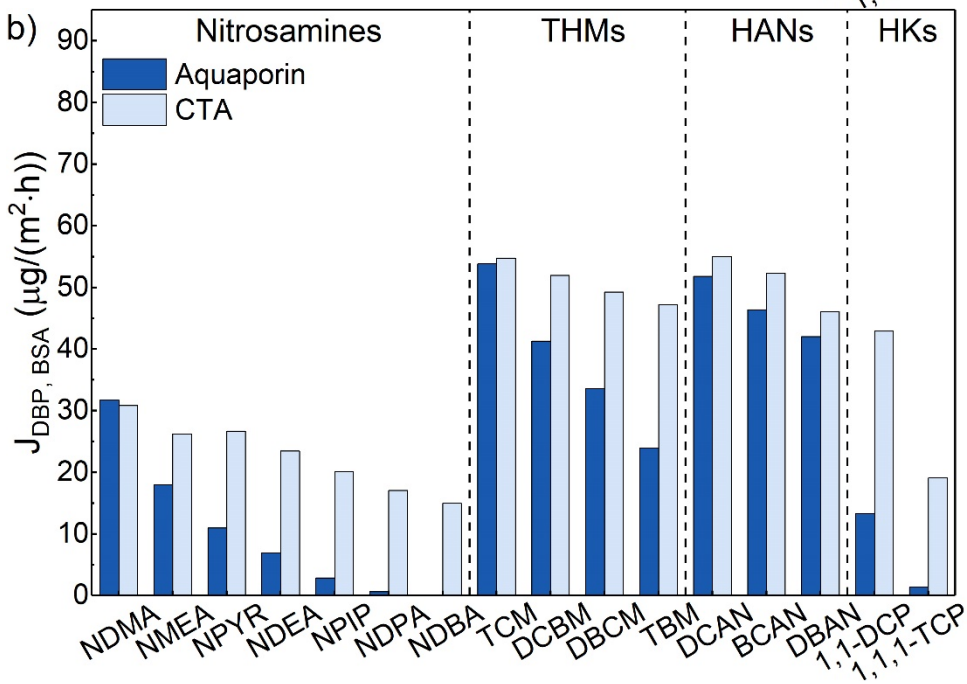
b)
Nitrosamines
THMs
HANs
HKs
Aquaporin
CTA
$J_{DBP, BSA}$ (μg/(m²·h))
0
10
20
30
40
50
60
70
80
90
NDMA
NMEA
NPYR
NDEA
NPIP
NDPA
NDBA
TCM
DCBM
DBCM
TBM
DCAN
BCAN
DBAN
1,1-DCP
1,1,1-TCP

54

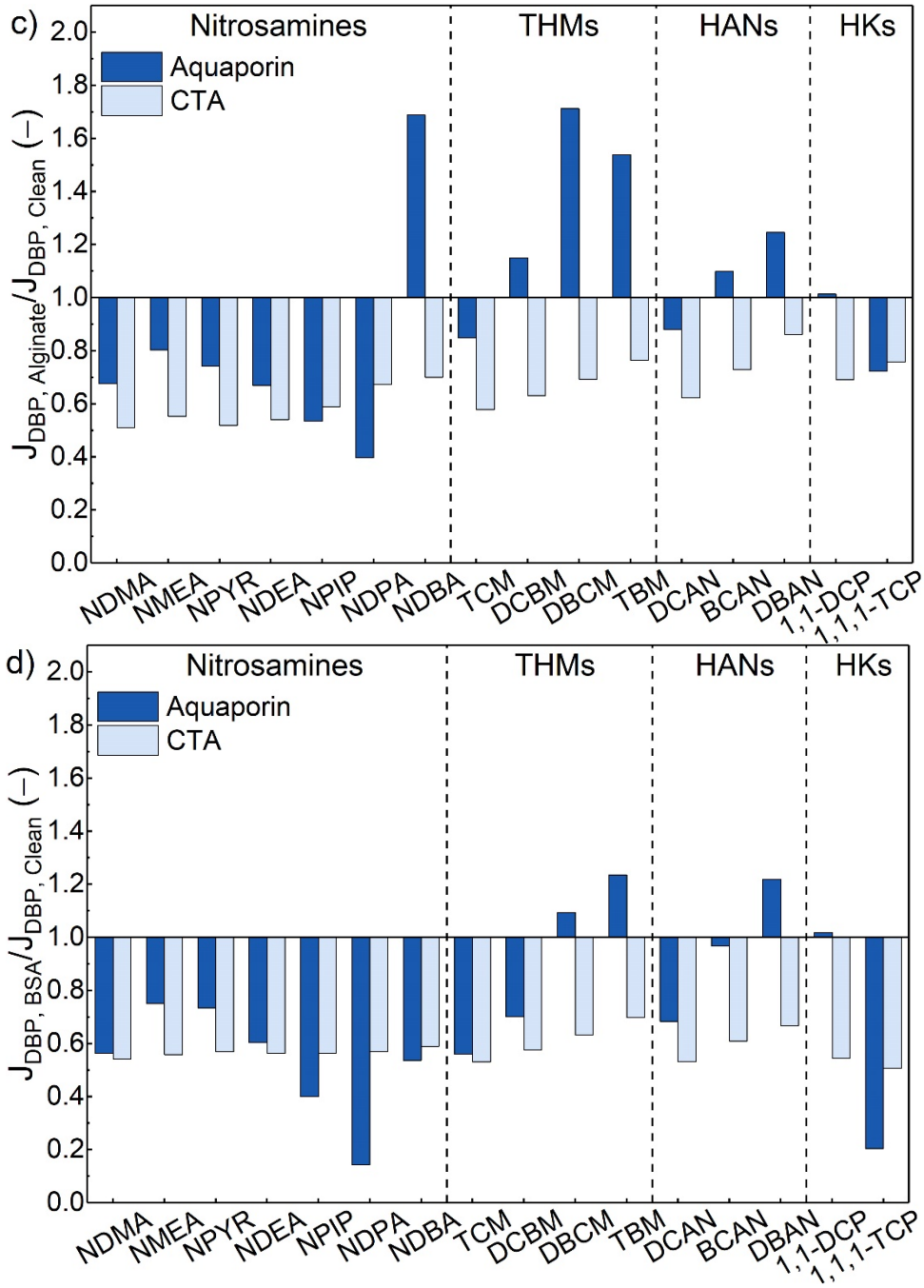

Figure SI-10. DBP fluxes of nitrosamines and halogenated DBPs by (a) alginate- and (b) BSA-fouled membranes; relative difference of DBP fluxes through (a) alginate- and (b) BSA-fouled membranes compared to clean membranes. Water fluxes for alginate-fouled membranes were 5.7 and 3.6 L/(m^2·h) for Aquaporin and CTA, respectively; water fluxes for BSA-fouled membranes were 3.8 and 3.2 L/(m^2·h) for Aquaporin and CTA, respectively; draw solution 1 M NaCl; nitrosamine concentration 10 µg/L; halogenated DBP concentration 20 µg/L; temperature 21 °C; solution pH 6.5–7.5. Relative difference of DBP fluxes were calculated based on data from Figure 3 in the main text.

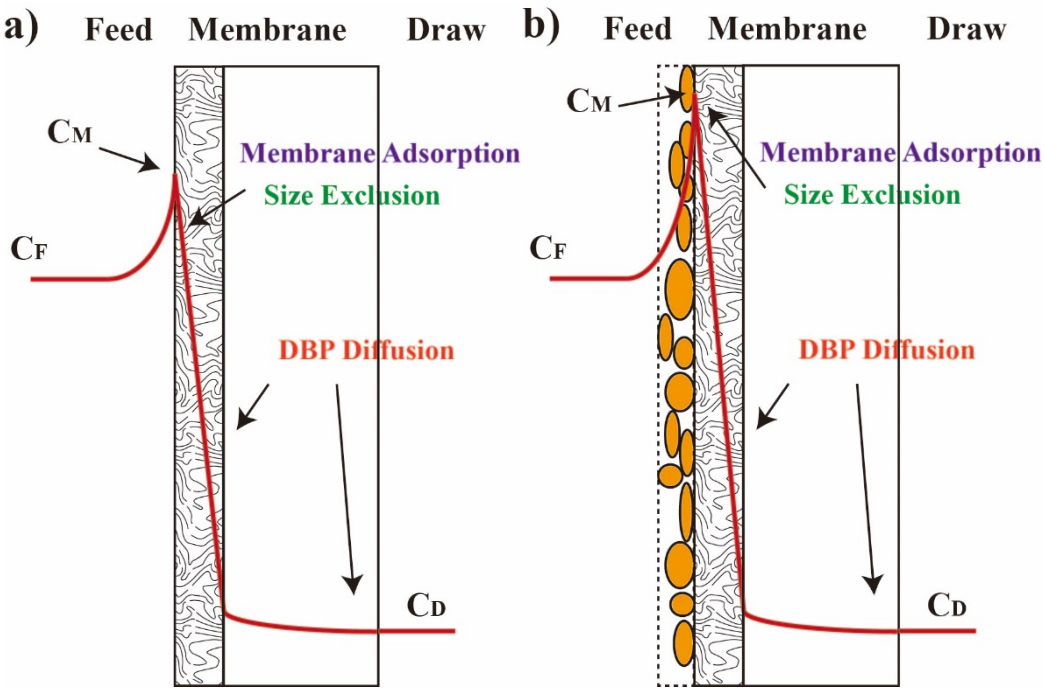

Figure SI-11. DBP concentration profile in FO with (a) clean and (b) fouled membranes. C_F feed concentration; C_M membrane surface concentration; C_D draw concentration.

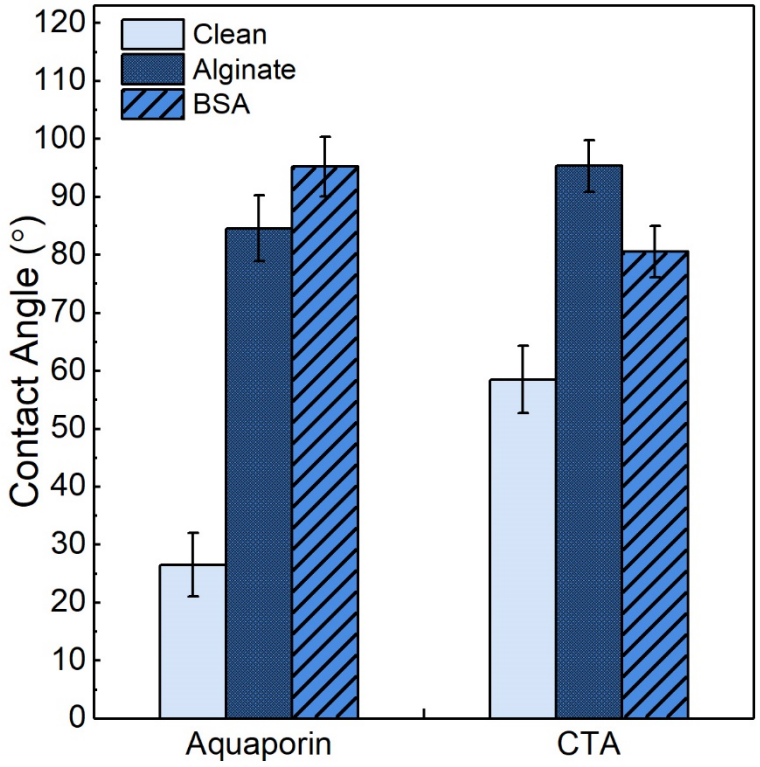

Figure SI-12. Water contact angles of Aquaporin and CTA membranes with and without fouling by alginate and BSA. Error bars represent the standard deviation from multiple replicates experiments.

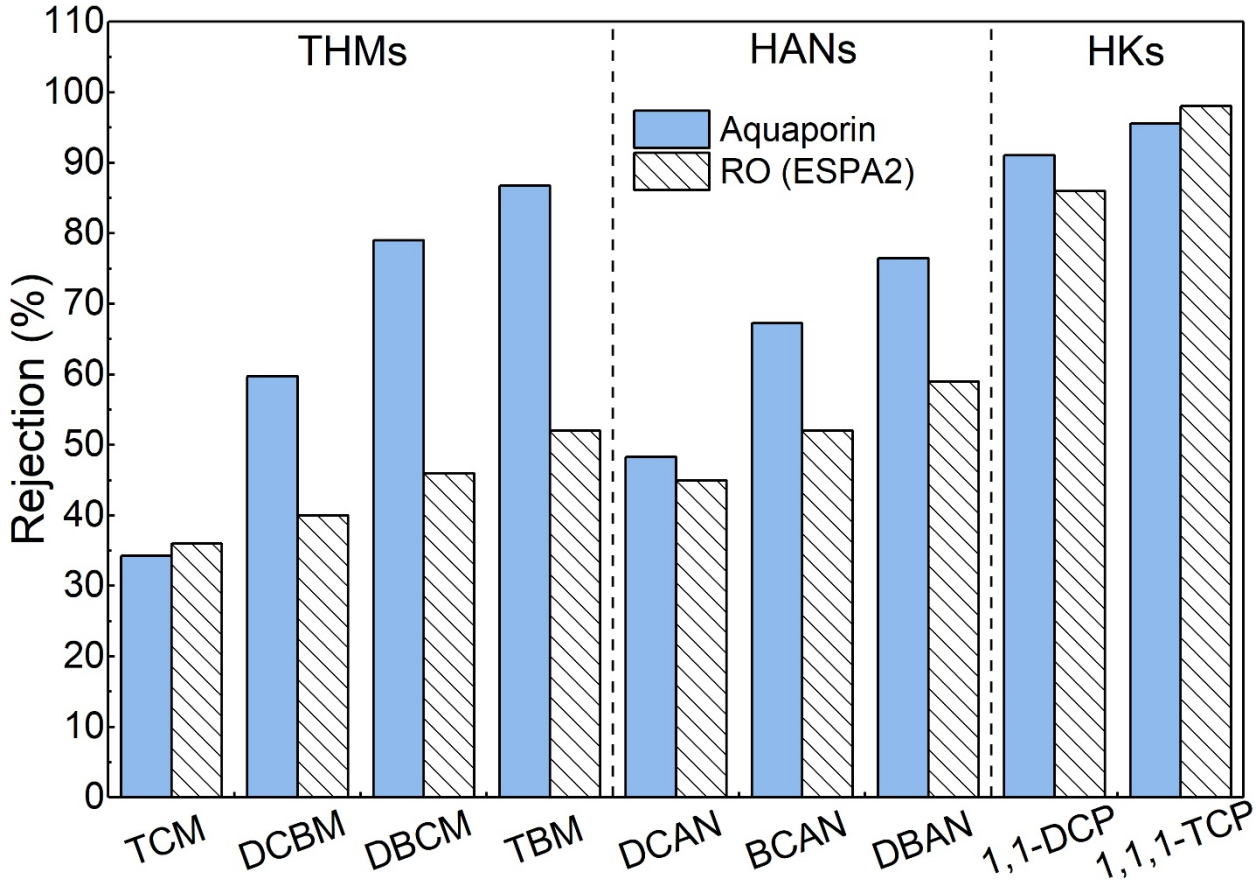

Figure SI-13. Comparison of the rejection of halogenated DBPs by Aquaporin membrane in FO and by ESPA2 membrane in RO [12]. Water fluxes for Aquaporin and ESPA2 were 8.1 and 18 L/(m^2·h), respectively. FO experiment: draw solution 1 M NaCl; DBP initial concentration 20 µg/L; temperature 21 ^{o}C; solution pH 6.5–7.5.

References

[1] M. Shakaib, S.M.F. Hasani, M. Mahmood, CFD modeling for flow and mass transfer in spacer-obstructed membrane feed channels, J. Membr. Sci. 326 (2009) 270-284.

[2] M. Xie, L.D. Nghiem, W.E. Price, M. Elimelech, Comparison of the removal of hydrophobic trace organic contaminants by forward osmosis and reverse osmosis, Water Res. 46 (2012) 2683-2692.

[3] M. Xie, W. Luo, H. Guo, L.D. Nghiem, C.Y. Tang, S.R. Gray, Trace organic contaminant rejection by aquaporin forward osmosis membrane: Transport mechanisms and membrane stability, Water Res. 132 (2018) 90-98.

[4] C. van Oss, Interfacial Forces in Aqueous Media, Second Edition, CRC Press, 2006.

[5] L.L. Xia, M.F. Andersen, C. Helix-Nielsen, J.R. McCutcheon, Novel commercial aquaporin flat-sheet membrane for forward osmosis, Ind. Eng. Chem. Res. 56 (2017) 11919-11925.

[6] Z.Y. Li, R.V. Linares, S. Bucs, L. Fortunato, C. Helix-Nielsen, J.S. Vrouwenvelder, N. Ghaffour, T. Leiknes, G. Amy, Aquaporin based biomimetic membrane in forward osmosis: Chemical cleaning resistance and practical operation, Desalination 420 (2017) 208-215.

[7] H.T. Madsen, N. Bajraktari, C. Helix-Nielsen, B. Van der Bruggen, E.G. Sogaard, Use of biomimetic forward osmosis membrane for trace organics removal, J. Membr. Sci. 476 (2015) 469-474.

[8] N.Y. Yip, A. Tiraferri, W.A. Phillip, J.D. Schiffman, M. Elimelech, High performance thin-film composite forward osmosis membrane, Environ. Sci. Technol. 44 (2010) 3812-3818.

[9] C. Boo, S. Lee, M. Elimelech, Z. Meng, S. Hong, Colloidal fouling in forward osmosis: Role of reverse salt diffusion, J. Membr. Sci. 390-391 (2012) 277-284.

[10] J. Wei, C. Qiu, C.Y. Tang, R. Wang, A.G. Fane, Synthesis and characterization of flat-sheet thin film composite forward osmosis membranes, J. Membr. Sci. 372 (2011) 292-302.

[11] W.M. Deen, Hindered transport of large molecules in liquid-filled pores, Aiche J. 33 (1987) 1409-1425.

[12] A.R.D. Verliefde, E.R. Cornelissen, S.G.J. Heijman, E.M.V. Hoek, G.L. Amy, B.V.d. Bruggen, J.C. van Dijk, Influence of solute−membrane affinity on rejection of uncharged organic solutes by nanofiltration membranes, Environ. Sci. Technol. 43 (2009) 2400-2406.